



Technical Memorandum

TITLE: Post-Well Subsurface Description of Macondo well (MC0252_1BP1) v3

TO: Kate Baker, Cindy Yeilding, Jay Thorseth, Peter Carragher

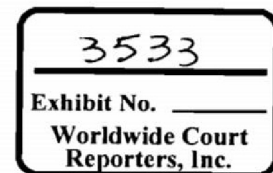
WRITTEN BY: Marty Albertin, Chuck Bondurant, Kelly McAughan, Binh van Nguyen
Bryan Ritchie, Craig Scherschel, Galina Skripnikova

DATE: 26th July 2010

Introduction

This technical memorandum outlines the post-well subsurface description of the Macondo well in Mississippi Canyon Block 252 (OCS-G-32306) in the north-central Gulf of Mexico.

Prospect Name	Macondo
Surface Location Block No.	Mississippi Canyon 252
BP well name	MC 252_1
OCS-G Well number	OCS – G32306_01
Spud date on Marianas	6 th October 2009
Released Marianas due to Hurricane Ida	27 th November 2009
Re-entered well on Deepwater Horizon	10 th February 2010
Category (Expl/Appr)	Exploration
Total Depth (MD/TVD/TVSS)	18,360' md / 18,349' tvd / -18,274' tvdss
EP Approved by MMS	6 th April 2009
Water Depth	4,992 feet
Rotary Table Elevation	75 feet RKB



Version 1

BP Confidential

1

CONFIDENTIAL

BP-HZN-BLY00082874
BP-HZN-BLY00082874

TREX 003533.0001

Macondo spud

October 6, 2009

Marianas pulled off location

November 27, 2009

After running the 18" casing and cementing the same, the Marianas BOP failed a scheduled test. At the time of the failed test, the 18" casing had been run and cemented. No open hole was exposed. A cement plug was set in the 28" casing, and the riser/BOP stack was pulled. While the BOP stack was being repaired on deck, the late season hurricane Ida formed in the gulf. The well location was in the projected path of the hurricane. The Marianas was evacuated. Upon returning to the rig after the storm, inspections had revealed extensive damage to wire/cables along the underside of the rig. These wires/cables were damaged as the result of waves/swells impacting the underside of the hull. This caused the sheathing of many of the wires/cables to be worn to the point that bare wires were exposed. After assessing the situation it was deemed that the damage was too extensive to perform repairs on location. The rig was de-moored and towed to a shipyard in Mississippi to perform the requisite repairs. While being repaired in the shipyard, the rig contract expired. After finishing repairs, the rig was released.

Well status at time the Marianas was pulled off location

The 18" casing was run and cemented. A 200' cement plug was set near the 28" casing shoe. It was decided that the Deepwater Horizon would finish drilling the Macondo well after finishing appraisal drilling operations at the Kodiak discovery.

On location with the Deepwater Horizon

January 31, 2010

After performing scheduled drawworks and BOP maintenance, running the riser, and testing the BOP on the wellhead, the Macondo well was re-entered on February 10, 2010. Upon re-entry, the cement plug set by the Marianas was drilled-out. After squeezing the 18" casing shoe, the Deepwater Horizon began making new hole on February 15, 2010.

Date encountered and depth of main target

The primary M56 target was encountered on April 4, 2010 while drilling at a depth of 18,065' (MD)/18,054' (TVD).

Date and depth of final TD

The Macondo well reached a final TD of 18,360' (MD)/18,349' (TVD) on April 9, 2010.

Post-TD operations

After reaching TD, a full suite of wireline evaluation was performed. There were wiper trips during the logging operations but there was a wiper trip after the logging was completed. Following wireline operations, production casing was run and cemented on April 18-20. At the time of the incident, the riser was being displaced to seawater in preparation to unlatch from the wellhead and pull the riser/BOP stack.

Geological description

The primary target for the Macondo well was an amalgamated low relief channel-levee system of Middle Miocene age (M56 ~13Ma) (Figure 1). The channel system trends in a north-west to south-east direction over an elongated Mesozoic 4-way ridge that strikes north-east to south-west. The trapping elements are a combination of dip and stratigraphic. The depositional system is interpreted to be low relief channel-levee deposits.

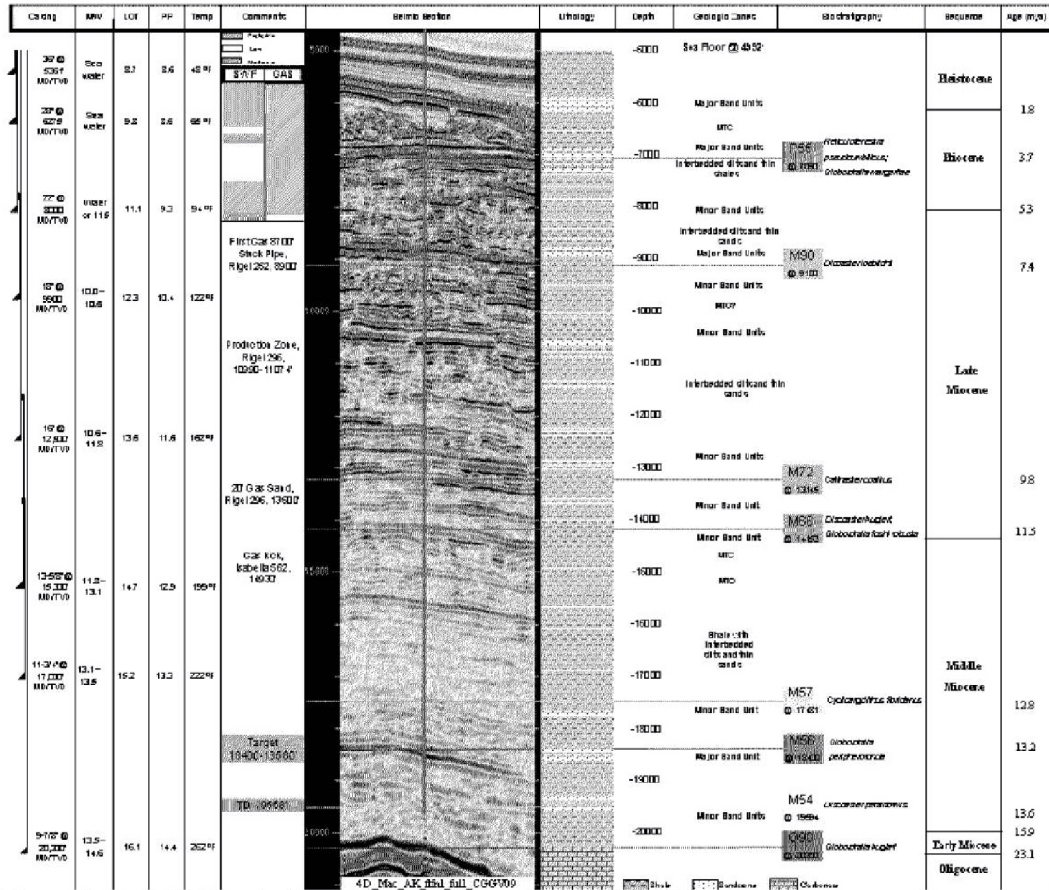


Figure 1: Pre-drill lithostratigraphy and drilling plan for MC0252_1 well.

The log signature and naming convention for the sands below the 9-7/8" liner that were penetrated by the MC0252_1BP1 well are shown in Figure 2. The depth structure and amplitude maps for the M56 and M57 intervals are shown in Figures 3 and 4.

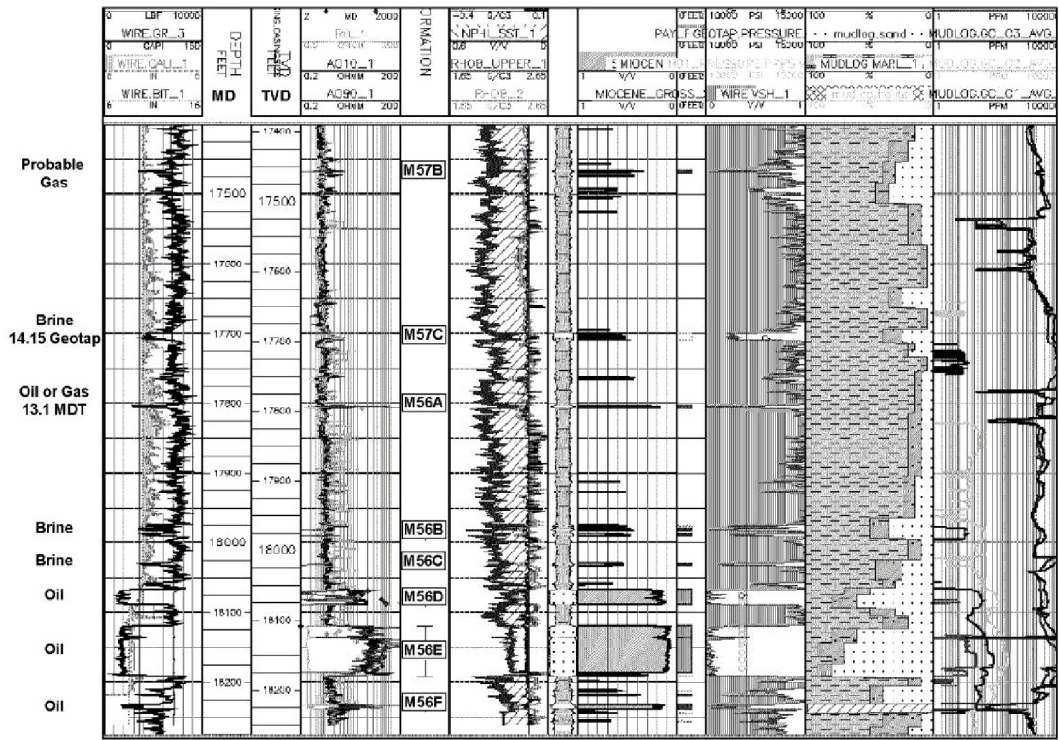


Figure 2: Sand identification chart for sands below the 9-7/8" liner that were penetrated by the MC0252_1BP1 well.

M56 Depth and Brine/Oil Distribution Maps

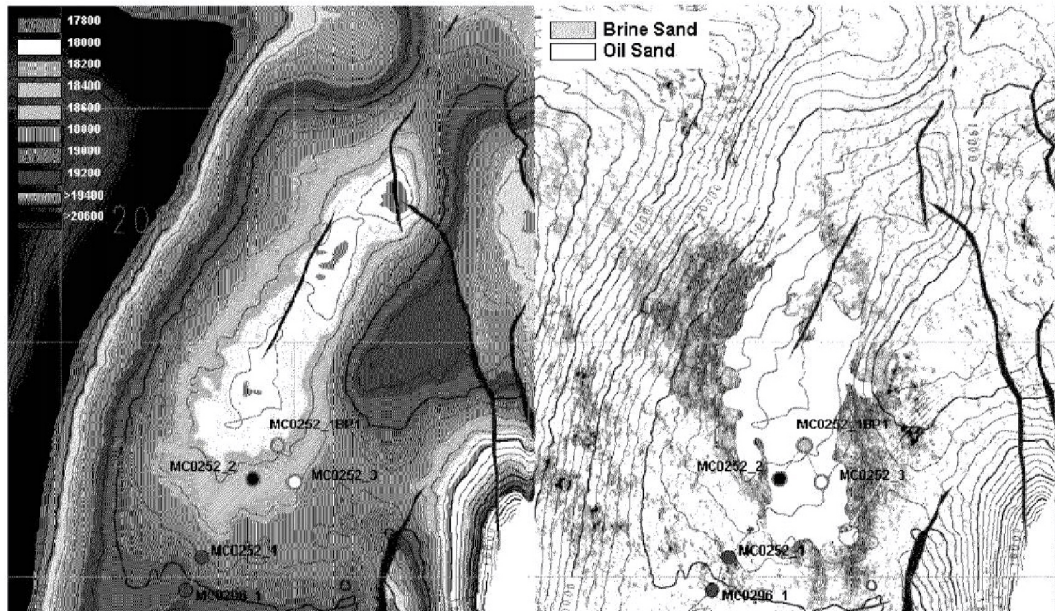


Figure 3: M56 Depth Structure Map and Amplitude Map of Channel System (Note: Seismic does not have the resolution to identify individual channels at this depth).

Rigel field

1 to 3 miles to the south-west of the Macondo well is a series of five channel-levee complexes. These channel sands range in depths from 9100ft TVDSS to 14,000ft TVDSS. The Rigel field produces biogenic gas from one of the channel systems (Figure 5).

The Rigel field is a shallow (~11,000') biogenic gas field in south-central Mississippi Canyon block #252. It is approximately M72 in age. The original Rigel exploration well was drilled by Texaco in 1999 to a TD of 13,600' (MD)/12,832' (TVD). Subsequently, a production well was drilled in 2003 by Dominion E&P. This well reached a TD of 16,200' (MD)/14,162' (TVD). This well is drilled from block 252 directionally toward the southwest. The bottom-hole location is in Mississippi Canyon block #296. This well is completed in a single zone around 11,000' (TVD). As of the middle of last year, the well has produced 72.5bcf dry gas. It is exported via the Rigel pipeline. The well is currently operated by ENI.

Seismic evidence shows that the lateral extent of the closest of these channel-levee systems (M110) does not reach the Macondo well (Figure 6).

M57 Depth and Brine/Oil Distribution Maps

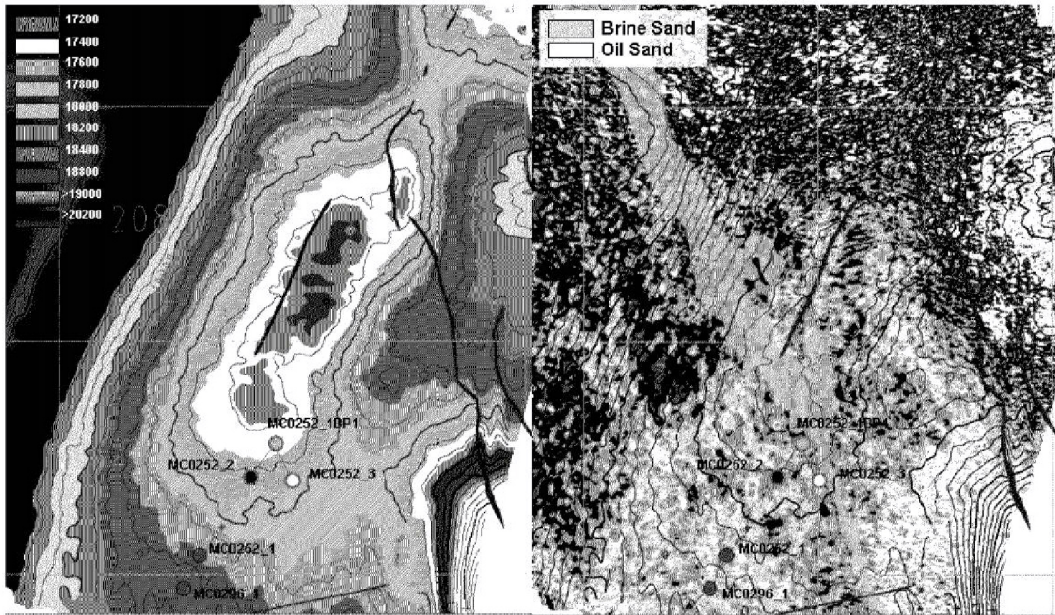


Figure 4: M57 Depth Structure Map and Amplitude Map of Channel System (Note: Seismic does not have the resolution to identify individual channels at this depth).

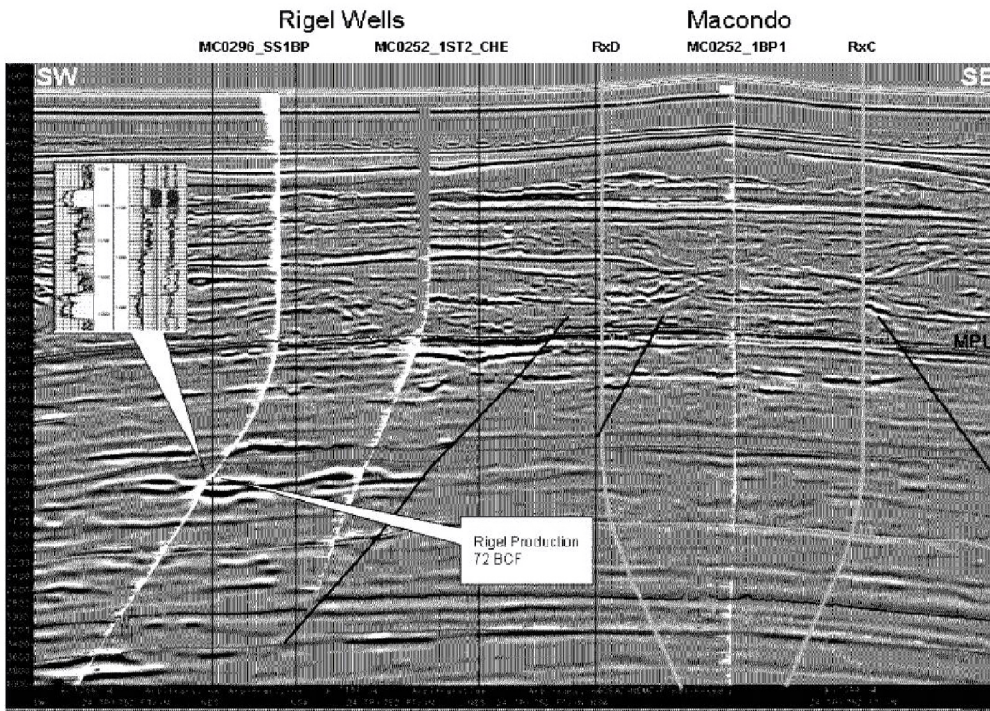


Figure 5: Seismic section showing Rigel wells and Macondo.

Version 1

BP Confidential

6

CONFIDENTIAL

BP-HZN-BLY00082879

BP-HZN-BLY00082874

TREX 003533.0006

M110 Depth and Brine/Oil Distribution Maps

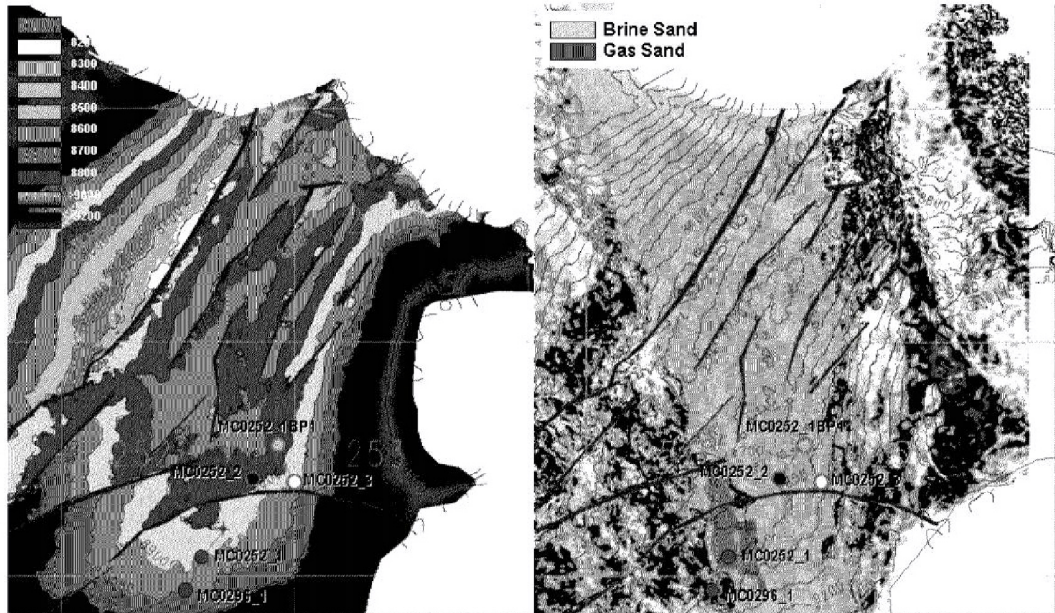


Figure 6: M110 Depth Structure Map and Amplitude Map of Channel System (Note: Seismic does not have the resolution to identify individual channels at this depth).

Shallow Hazards

BP completed an archaeological and seafloor geohazards survey across Mississippi Canyon Block 252 and vicinity in January 2009 to meet MMS requirements for archaeologically significant blocks. No significant man-made or natural hazards were identified near the proposed MC 252-1 well or within the proposed anchor radius for the Marianas drilling rig.

The shallow hazards discussion is limited to the top-hole or riserless section (i.e. between seafloor and the base of the 22-inch casing section). Figure 7 shows the top-hole formation forecast (THFF) for shallow geohazards that was derived from 3D seismic data. Figure 8 shows the shallow hazards top-hole observations log that was generated after drilling the top-hole section. The post-well comparison between actual drilling conditions and pre-drill prediction is provided below.

Shallow Gas

The zone from the seafloor to 8,001 ft MD (base of 22-inch casing section) was predicted to have a Negligible potential of shallow gas. No shallow gas was observed while drilling the riserless section.

Shallow Water Flow

A Low risk for SWF was assessed for two intervals (6,570 ft to 6,701 ft MD and 7,025 ft to 7,614 ft MD). There was one unit predicted with a Moderate risk of encountering SWF in the pre-drill THFF between 6,913 ft and 7,025 ft MD. Although sand-prone intervals are noted from the gamma log between 6,660 ft to 6,900 ft and 6,950 ft to 7,080 ft, no SWF was noted while drilling the riserless section.

A slight flow was noted across the top of the wellhead about 50 hrs after reaching the total depth (TD) of the 22-inch casing section while tripping in hole with the 22-inch casing. It is assumed that the slight flow may have come from possible sands noted above. The flow was stopped by circulating mud.

Hydrates

The potential for gas hydrates was predicted as Negligible-Low for the entire riserless section. There was no visual evidence or log data that indicated possible gas hydrates while drilling the riserless section.

Gumbo

The potential for gumbo shale, a plastic clay return response to water based mud, was not addressed in the pre-drill THFF. This was not a concern because the plan was to drill the hole section with seawater. Gumbo was observed towards the end of drilling the 22-inch casing hole section. The gumbo coincided with circulating pad mud in place in preparation for running casing.

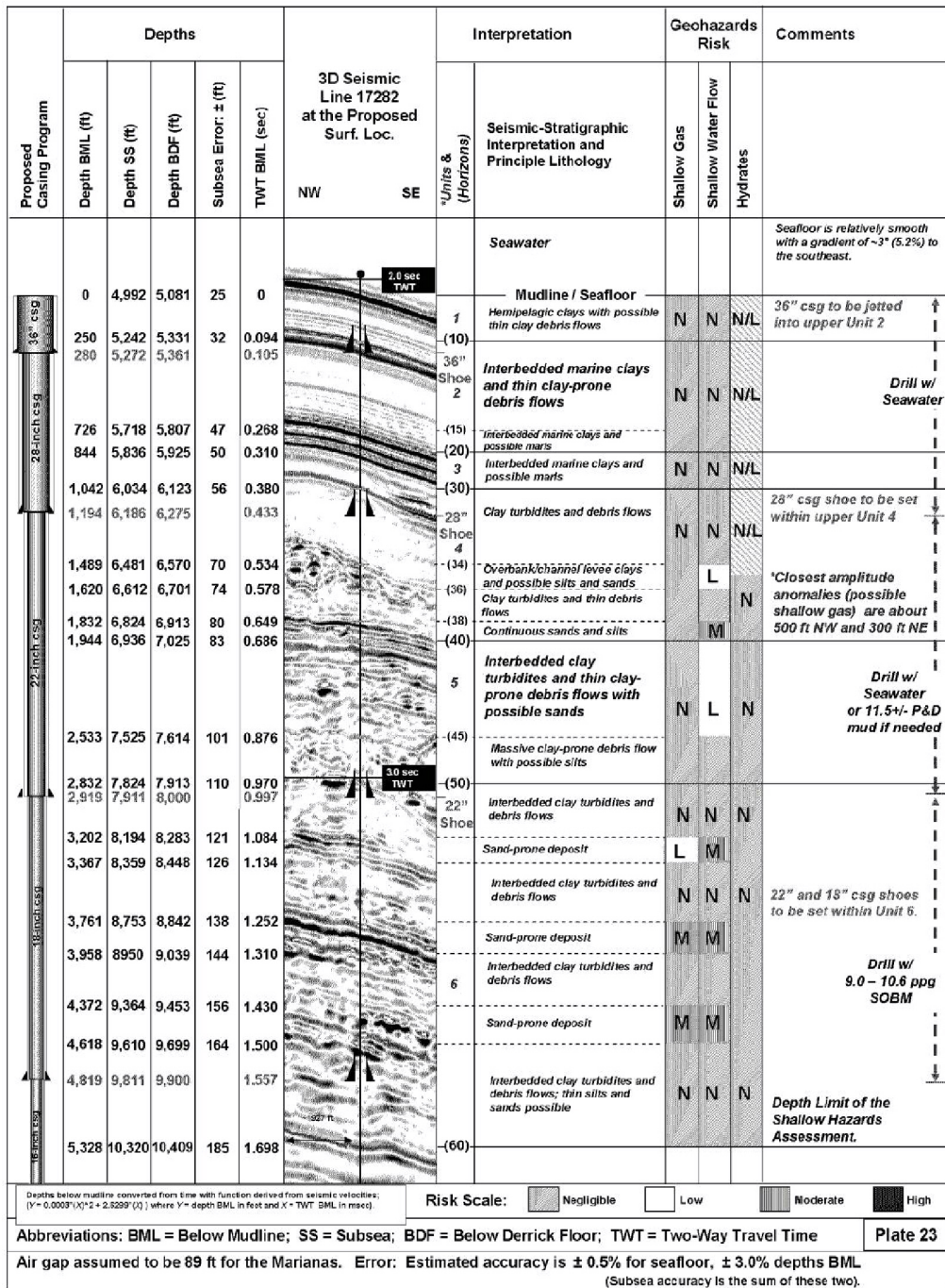


Figure 7: Original Top-Hole Formation Forecast at the Proposed MC-252 #1 Location (produced by Craig A. Scherschel, 08 June 2009).



MC 252 #1 (Macondo) LWD Log with Shallow Hazards Observations

WELL LOCATION: Proposed MC 252 Location
 AREA: Mississippi Canyon 252
 WELL APT: 5081741169 00
 DATE: 6-10 Oct 2009

EASTING: 1 202 798 93 FT
 NORTHING: 10 431 819 79 FT
 DATUM: NAD 1927, Spheroid: Clarke 1866
 PROJECTION: UTM Zone 18N (1)

Pre - Drill Assessment
 Predicted Subsea Depth

Water Depth = 4,992' SS

Post - Drill Observations
 Measured Depth (Air Gap - 89 ft)
 Water Depth = 4,992' SS

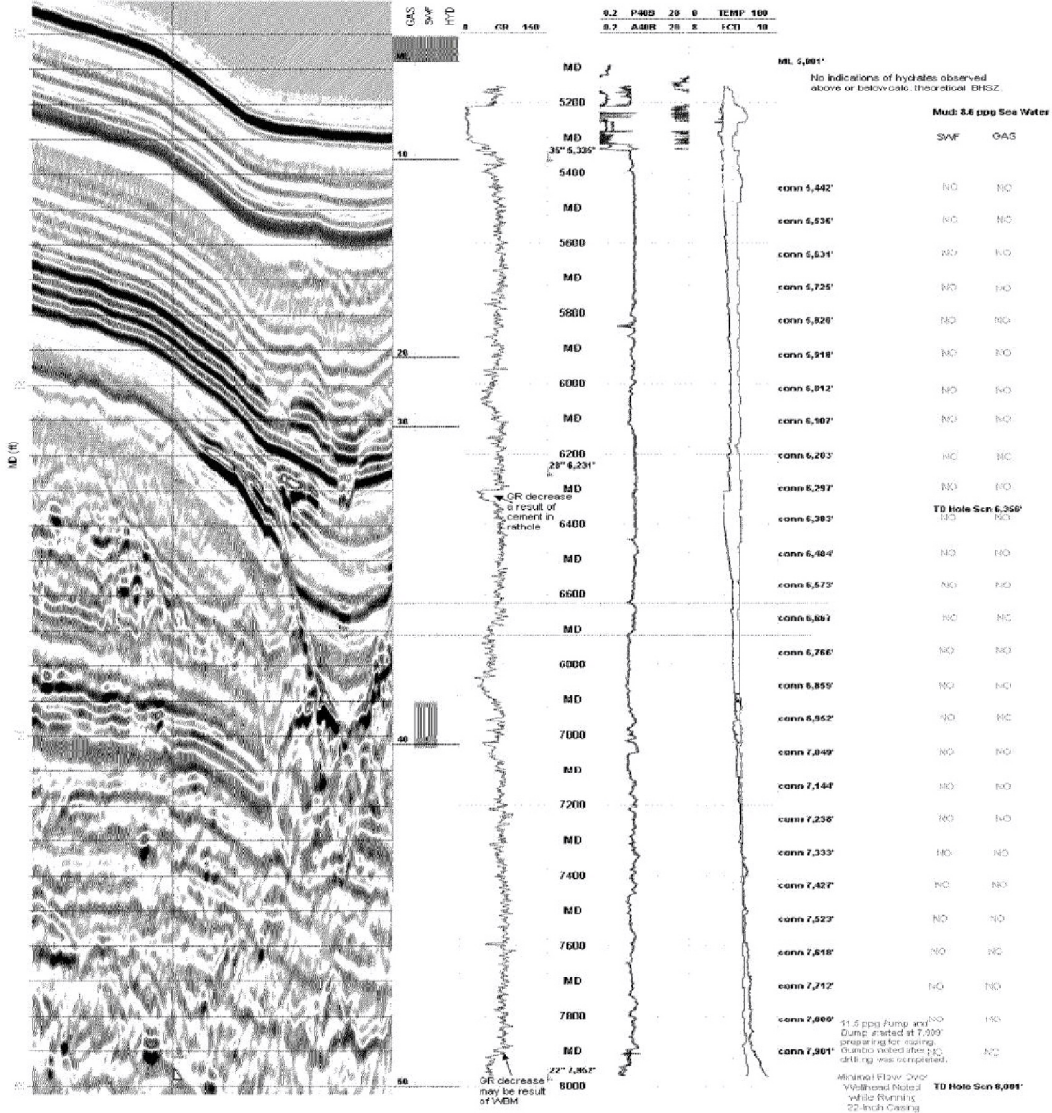


Figure 8: Shallow Hazards Top-hole Observations Log for the MC-252 #1 Location between Seafloor and the Base of the 22-inch Casing Hole Section (produced by Kate Paine, October 2009).

Pore Pressure and Fracture Gradient

The current interpretation of pore and fracture pressure at Macondo incorporates revisions to the pre-drill forecast based on: synthesis of LWD and wireline pressure indicators (pressure transforms based on resistivity, sonic, checkshot, and density); drilling parameters and data (D-Exponent, background, and connection gases); and direct drilling indicators (kicks, losses, and real-time/wireline direct pressure measurements), Figure 9. Pore pressure is interpreted to be higher than the predrill most likely curve from 9000' to 17750' TVDKB. This is due to slower than predicted interval velocities and revised pressure transform parameters more similar to those required to reconcile pressure measurements and indirect pressure estimates from logs at the high pressure, narrow margin offset well "Yumuri", MC382-1. Reservoir pressures at Macondo are much lower than predicted – pressure in the oil bearing reservoir sands represent the only interval which falls outside of the pre-drill minimum-maximum pressure envelope. Pre-drill centroid modeling of channel sands draped over the large 4-way Macondo structure placed reservoir pressures 0.1-0.3 ppg higher than shale pressure. Actual reservoir pressures (similar reservoir pressure to Isabella) imply regional hydraulic connectivity, at least on a geologic time scale, to deeper water lower overburden/pore pressure environments to the south, or local connectivity updip beneath allochthonous salt bodies southwest and east of the prospect. Though wireline density is limited to the reservoir section, calibrated acoustic to density transforms of the Macondo sonic and checkshot imply that overburden is lower than predicted. Lower densities used in the calibrated postwell overburden are consistent with the higher than predicted pore pressure observed at the prospect. The narrow PPFG window above reservoir level, and weak formations exposed at the 22" shoe, led to shallower than planned casing depths, and the use of contingency liners.

Macondo MC_252-1-A Pressure Forecast: REV3 , 5/17/10

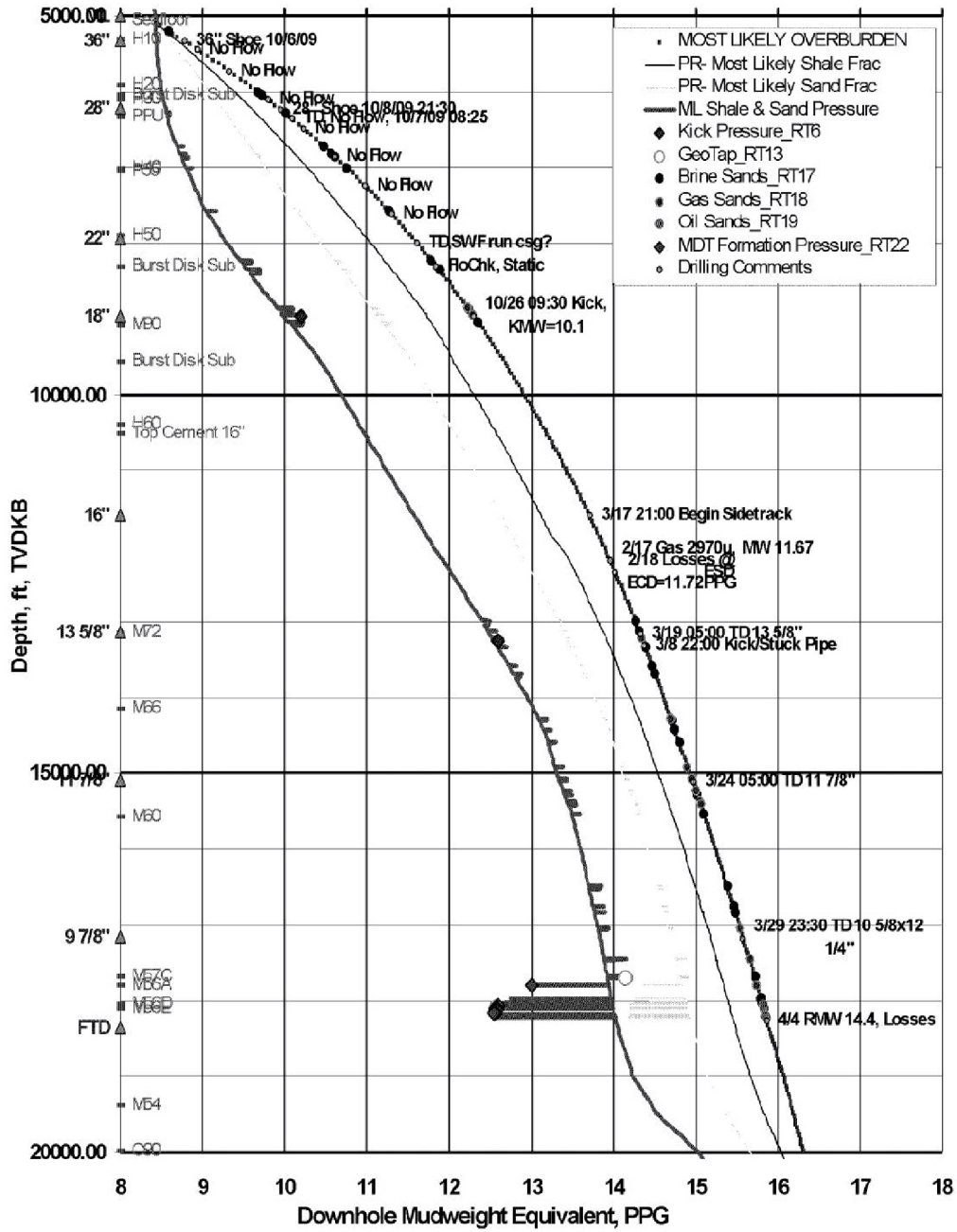


Figure 9: Post-well PPFG interpretation.

Petrophysics

Summary

From shows, log response and fluid samples it is interpreted that >90 feet of hydrocarbons were discovered by the Macondo well, the majority occurring in the M56D (22') and M56E (64.5') sands. Porosity averages 22%, Sw averages 10 - 17% and permeability averages in the range of 250 - 500 mD (arithmetic, log derived). Permeability was calculated using a porosity-permeability transform based on Macondo well rotary side wall core data analysis.

Three MDT multiphase fluid samples were collected. MDT sample analysis and PVT analysis confirm low OBM contamination level (0-1.2%) The samples were characterized as volatile oil with GOR ~3000 scf/stb, API 35 degrees, and viscosity of 0.2 cp.

No hydrocarbon-water contacts were penetrated and no significant aquifer sandstone was observed.

Rotary side wall core data were used to calibrate log derived porosity and permeability at net confining stress. Log porosity was calculated from density log calibrated to side wall core porosity data measured at net confining stress. Permeability data was calculated from log porosity calculated using a porosity-permeability transform based on Macondo well rotary side wall core data analysis. Water saturation was calculated from log derived porosity and resistivity data. Log porosity tied to core porosity well, log derived permeability had reasonable match. There is no core calibration for water saturation yet.

Based on core measurement (lower porosity and permeability values and laser grain size analysis) M56D is probably slightly different rock type and more heterogeneous than M56E. Nuclear-magnetic resonance (CMR) and RT Scanner logs response also show higher rock anisotropy of M56D lobe (See Figure 33).

The close match of core and log derived porosities in the M56E sand gives a reasonably high degree of certainty around the petrophysical parameters despite the relative lack of core data in Figure 17. A greater degree of uncertainty exists in the more heterogeneous M56D sand. Further uncertainty exists in the thin minor hydrocarbon bearing intervals in M56 and M57. They were not covered by core data and are difficult to resolve with standard logging tools as they are less than 2.5 feet in thickness. The lowest M56F sand was not fully covered by logs.

Electrical properties, capillary pressure data and thin section analysis will be incorporated into the interpretation when available.

Data base

All Logging While Drilling (LWD), Wireline, Mud logging, Pressure and Core data were loaded into Geolog where formation evaluation was completed.

LWD

Halliburton was the LWD vendor. GR, Resistivity, Sonic and PWD tools were in the BHA while drilling plus Geotap formation pressure in the target section.

In the section of the hole logged with wireline tools, LWD was depth shifted to TCOMBO Gamma Ray. In cased hole section, where wireline Sonic in casing was run, LWD was shifted to it to match sonic response on LWD and wireline. From mudline to top of sonic in casing (~11,700' md) the depth shift was distributed.

Wireline

The following Schlumberger open hole wireline logs were run in 6 descents in open hole section from 17,150'-18,270' MD. They include the following tools:

R1D1: ZAIT-GPIT-LDS-CNL-GR-LEHQT
R1D2: CMR-ECS-HNGS-LEHQT
R1D3: Dual OBMI-GPIT-DSI-GR-LEHQT
R1D4: MDT-GR-LEHQT (pressure and samples)
R1D5: MSCT-GR-LEHQT (rotary side wall cores) was not fully successful; repeated as R1D7 after R1D6
R1D6: Quad VSI-GR-LEHQT

Well logs interpretation sequence

- *Well site interpretation based on log field prints (R1D1 and R1D2) identifying depth of the shallowest hydrocarbon-bearing interval in the open hole - April 13th, 2010.*
- *Post incident peer review identifying every possible permeable interval and its saturation type - April 21st, 2010.*
- *Schlumberger ELAN interpretation - May 3rd, 2010.*

Basic observation on logs and borehole condition:

- The hole has a diameter of 8.5" from TD of 18270' to 18,090' md and 9.875" from 18,090' md to the 9.875" casing due to the use of a hole opener assembly.
- This hole section was drilled with barite as a mud weighting material (~20 % of high gravity weight solids). This causes the density correction curve (DRHO) to read negative and also significantly affects the quality of the PEF curve.
- Run R1D1 was run ~7 days after the formation was drilled and 20 hours after the last circulation stopped. During that time the open hole was exposed to different kinds LCM materials to treat losses, below the 9.875" shoe and close to TD. The caliper indicates some wash outs in shales but mainly gauge hole in sandstone.

Core

There were 44 rotary side wall core samples recovered from 3 MSCT runs. Sample preparation and analyses were done at Weatherford's Laboratories in Houston.

Only around 2/3rds of the samples were in a condition suitable for petrophysical analysis. After sufficient cleaning and drying, 6 samples were dedicated for mechanical properties and pore compressibility studies. 19 samples were selected for Routine Core Analysis (RCA). The analyses from 17 samples from M56D and M56E have been completed to date and are referenced in this document whilst 2 more sample are still being analysed. RCA was performed at 500 psi and at Net Confining Stress (NCS) of 2000 psi. NCS was calculated from post well sand fracture evaluation, over burden estimation and pore pressure.

If the assumption is made that one sample describes one inch of rock, the core plus represent approximately 2% of the M56D unit and 1.4% of the M56E in terms of amount of interval covered.

Currently Special Core analysis (Electrical Properties and Capillary pressure measurements) are planned to be run on a sub-set of samples. As of July 27th 2010, the samples are in the Weatherford Laboratories in Houston. The SCAL measurements are on hold as they have been subpoenaed.

16 out of the 17 samples were described as fine to medium size grain sandstones, one as shale.

Laser Grain Size Analysis (LGSA) results on 17 samples (6 in M56D and 11 in M56E) are presented in Figures 10 and 11.

In Figure 10 Klinkenberg corrected permeability to air at NCS is plotted versus the percentage of different size particles in the sample. There is a clear relationship between sand content and permeability.

It appears that the M56D samples (green) have marginally more silt and less sand grain size particles than M56E samples (blue), though with the relatively small data set this may be a function of the sampling.

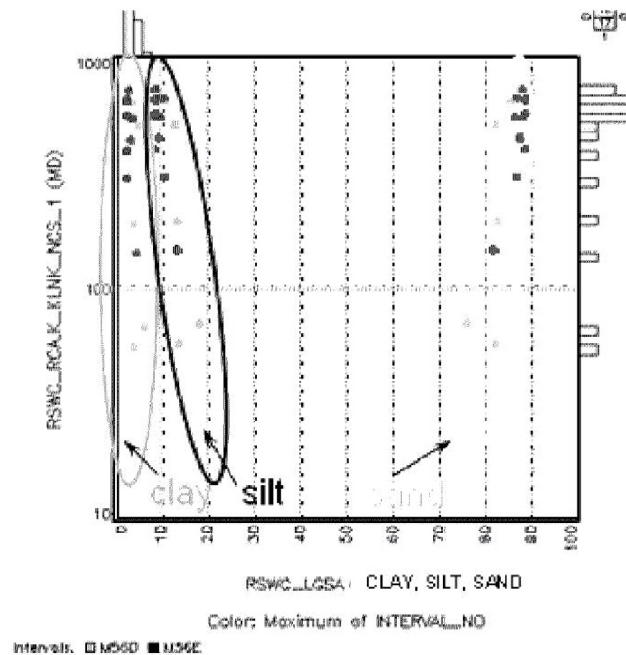


Figure 10: Laser Grain Size Analysis, Permeability vs. percentage of different (sand, silt, clay) size particles.

In Figure 11 Klinkenberg permeability to air at NCS is plotted versus percentage of different size sand particles. The data shows a clear relationship between grain size and permeability. In general M56D (green) has a subtly wider range of grain size suggesting slightly poor sorting, while the M56E (blue) is more homogeneous.

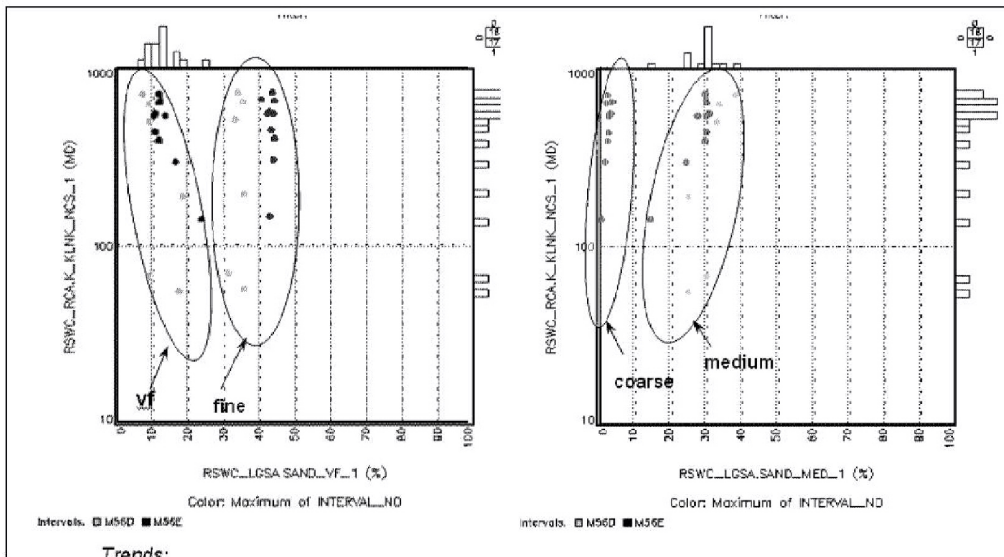


Figure 11: Laser Grain Size Analysis, Permeability vs. percentage of different (very fine, fine, medium and coarse) size sand particles.

The observations from Figures 10 and 11 leads to the suggestion that the M56E core plugs indicate slightly better sorting than the M56D plugs. This is reflected in their respective positioning in K/PHI space as indicated in Figure 12. Further the Winland iso-pore throat lines suggest that two sands may be slightly different rock types based on their degree of sorting. The 10 micron line divides the two rock type.

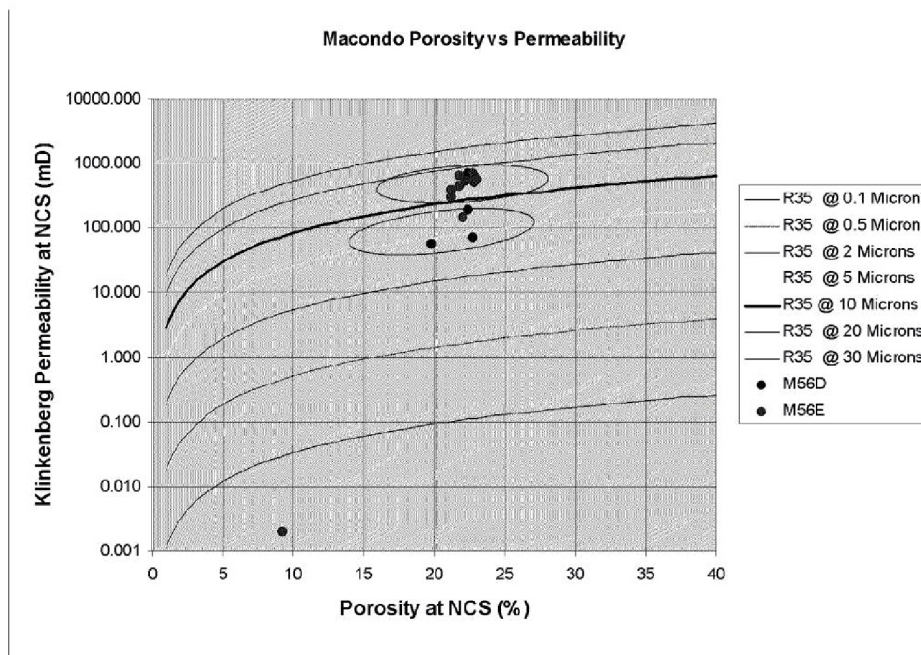


Figure 12: Winland R35 rock typing plot.

X-Ray diffraction (XRD) analysis results from 10 samples (4 in M56D and 6 in M56E) are presented in Figure 13. Mineralogical content of all analysed sandstone samples are in average 93% Quartz with Kaolinite (~2%) and Illite 1% clays, 1% K-spar and 3 % Plagioclase. Based on the 10 samples from M56D and M56E there appears to be no difference in mineralogy between the two sand bodies, so any variation in petrophysical properties is likely to be a function of grain size and most likely sorting.

WEATHERFORD LABORATORIES
X-RAY DIFFRACTION
(WEIGHT %)

FIGURE 13

Client: **BP America Production Company**
Well: **OCS-G-32306 No.1**
Area: **Mississippi Canyon Block 252**
Sample Type: **Rotary Sidewall Core**

Plug Number	Sample Depth (ft)	CLAYS				CARBONATES			OTHER MINERALS					TOTALS			
		Chlorite	Kaolinite	Illite	Mt. US*	Calcite	Dolomite	Siderite	Quartz	K-spar	Plag.	Pyrite	Zeolite	Barite	Clays	Carb.	Other
3-4R	18069.8	Tr	2	1	Tr	Tr	0	Tr	92	1	4	Tr	0	0	3	Tr	97
3-6R	18074.9	Tr	2	1	Tr	Tr	0	Tr	92	1	4	Tr	0	0	3	Tr	97
3-9R	18083.0	Tr	2	Tr	Tr	Tr	0	Tr	94	1	3	Tr	0	0	2	Tr	98
2-4R	18067.0	Tr	2	1	Tr	Tr	0	Tr	93	1	3	Tr	0	0	3	Tr	97
3-14R	18124.9	Tr	3	1	Tr	Tr	0	Tr	91	1	4	Tr	0	0	4	Tr	96
3-18R	18134.1	Tr	2	1	Tr	Tr	0	Tr	93	1	3	Tr	0	Tr	3	Tr	97
3-19R	18147.9	Tr	3	1	Tr	Tr	0	Tr	92	1	3	Tr	0	0	4	Tr	96
3-25R	18161.0	Tr	2	1	Tr	Tr	0	Tr	94	1	2	Tr	0	Tr	3	Tr	97
1-3R	18174.0	Tr	1	1	Tr	Tr	0	Tr	94	1	3	Tr	0	0	2	Tr	98
3-31R	18183.1	Tr	2	1	Tr	Tr	0	Tr	93	1	3	Tr	0	Tr	3	Tr	97
AVERAGE		Tr	2	1	Tr	Tr	0	Tr	93	1	3	Tr	0	Tr	3	Tr	97

Figure 13: X-Ray Diffraction Analysis. First 4 samples (from 3-4R to 2-4R) are for M56D, 6 next samples are from M56E.

Routine Core Analysis

After the rotary sidewall core plugs were cleaned and dried, the 17 samples were subjected to Routine Core Analysis (RCA). The measurements of porosity and permeability were performed at 500 psi and at 2000 psi (NCS). The analysis also included stair steps and repeat measurements of porosity and permeability.

Klinkenberg permeability to air at NCS is plotted versus Porosity at NCS in Figure 14. M56D sand may be more heterogeneous than M56E and its reservoir characteristics are hardly described by the available samples. More core data will be necessary for rock typing work. From the Laser grain analysis - sorting may be a function in this effect more than grain size.

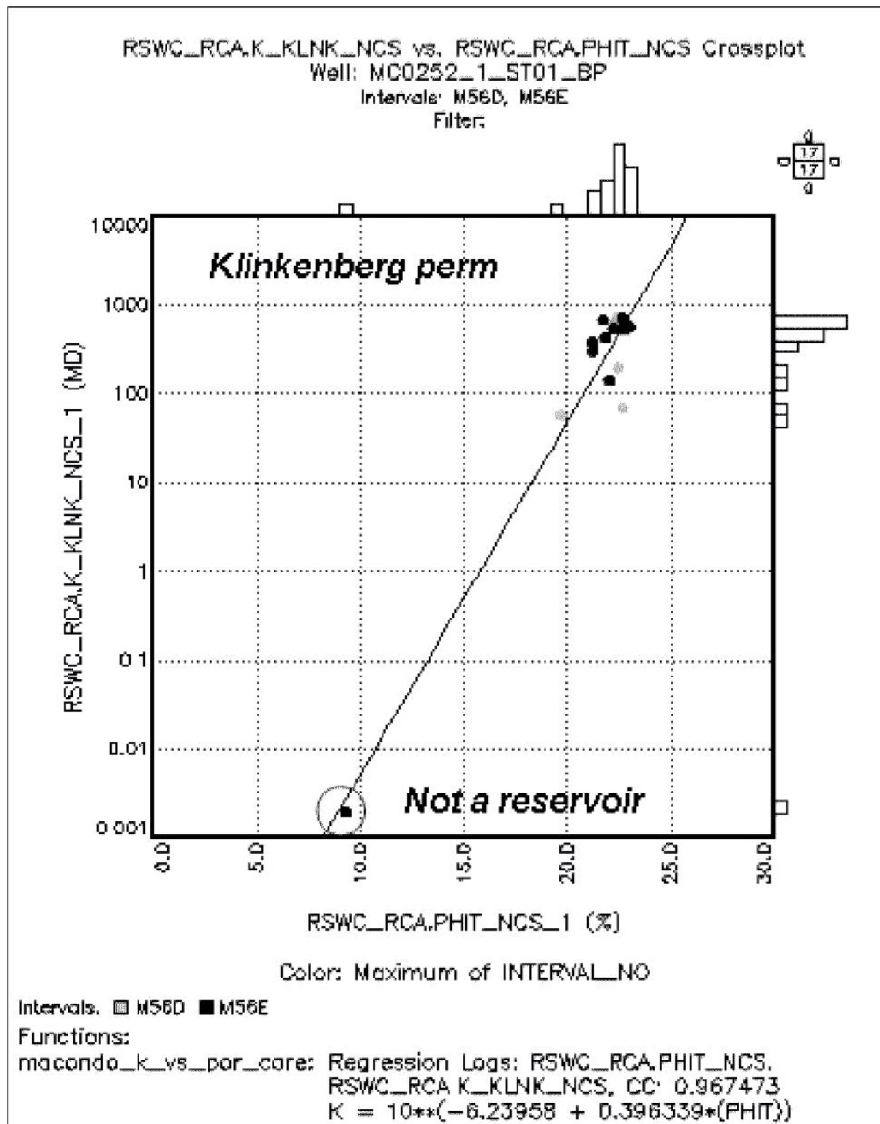


Figure 14: RCA Klinkenberg permeability to air at NCS is plotted versus porosity at NCS with linear regression function used for permeability calculation. Set of 17 samples is plotted.

Frequency histograms of core derived porosity and permeability are presented in Figure 15. The porosity of the M56D samples is very close to M56E samples. The permeability of the M56D samples is less than M56E samples. This may be due to sorting, packing, grain size distribution or combination of these factors. The mineralogical content of the M56D and M56E is interpreted to be similar. Given paucity of core data, the permeability variation of the two sands is not greatly significant (363 mD in M56E vs. 493 mD in M56D, see Figure 15).

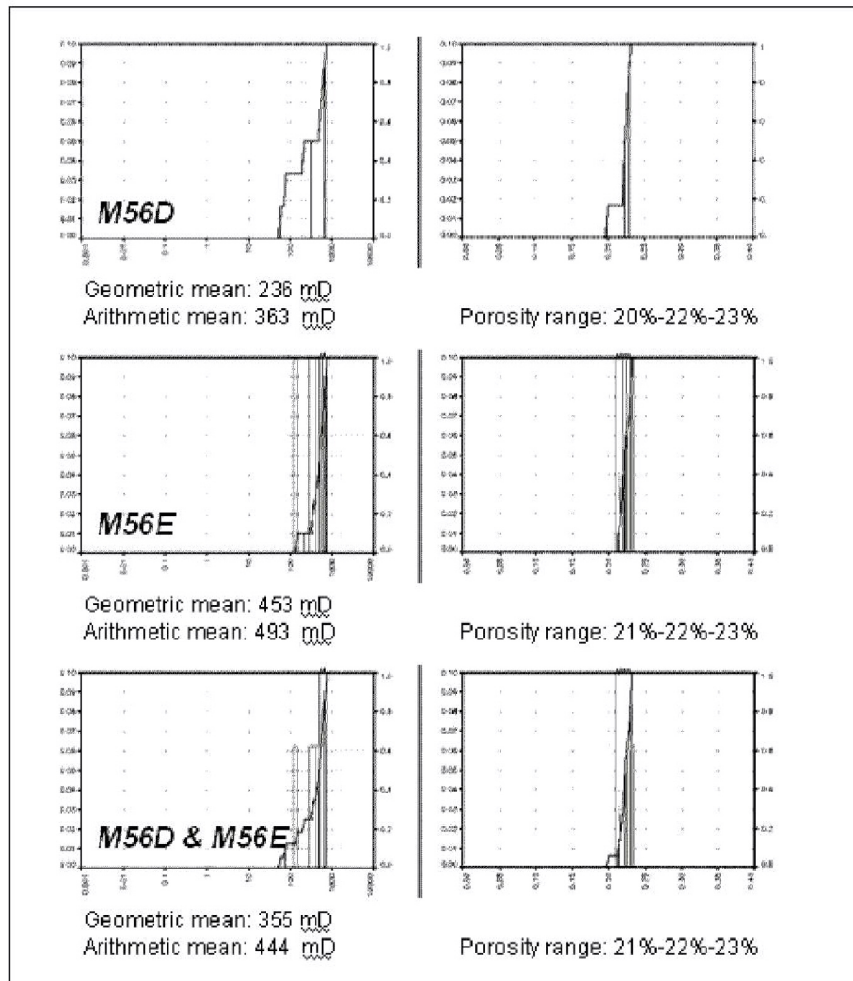


Figure 15: Frequency distribution of Core measured Klinkenberg permeability to air at NCS and Porosity at NCS separately per sands and both sands together.

Log to Core calibration

Porosity was derived from the density log from the following equation:

$$\text{Density porosity (dec)} = (\text{Rhog} - \text{Rhob}) / (\text{Rhog} - \text{Rhof})$$

Where:

- Rhog is grain density (g/cc)
- Rhob is the density log (g/cc)
- Rhof is the fluid density (g/cc)

Grain Density (Rhog) and Fluid Density (Rhof) were determined from core derived data.

Frequency distributions of core measured Rhog and log Density (Rhob) vs. core measured porosity (Phit_ ncs) plot are presented in Figure 16.

Core derived Rhog from the M56D and M56E sands are very similar at 2.645 g/cc. However the cross-plot of Core porosity v Density log (RhoB) shows the M56D sand plugs to plot off trend with the M56E plugs. The force fit line through the M56E plugs through the grain density of 2.645 g/cc gives a very reasonable Fluid density Rhof of 0.845 g/cc, which is consistent with the reservoir fluid from pressure data and the mud filtrate density. A number of M56D plugs suggest a higher Rhof of greater than 1 g/cc which is inconsistent with the reservoir fluids derived from logs, pressure data and fluid evaluation. Considering these data points to be anomalous, a RHOF=0.845 g/cc is used for Density porosity evaluation for all sands.

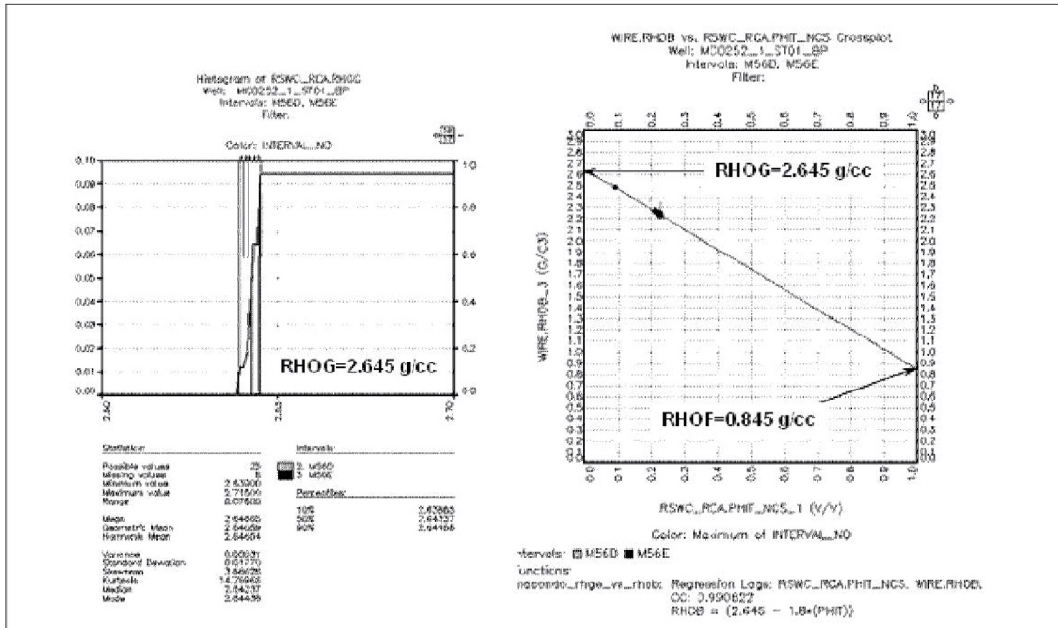


Figure 16: RCA. Core grain density distribution and Cross plot of Density log vs. Core porosity at NCS.

Figure 17 is an overlay of calculated density porosity core plug porosity. Core plugs were slightly shifted to logs, the original samples location on the left side of the Figure 17 with depth shifted plugs on the right side.

The depth shift is to better match the Density porosity and correct the misplacement of shale sample at 18,121'.

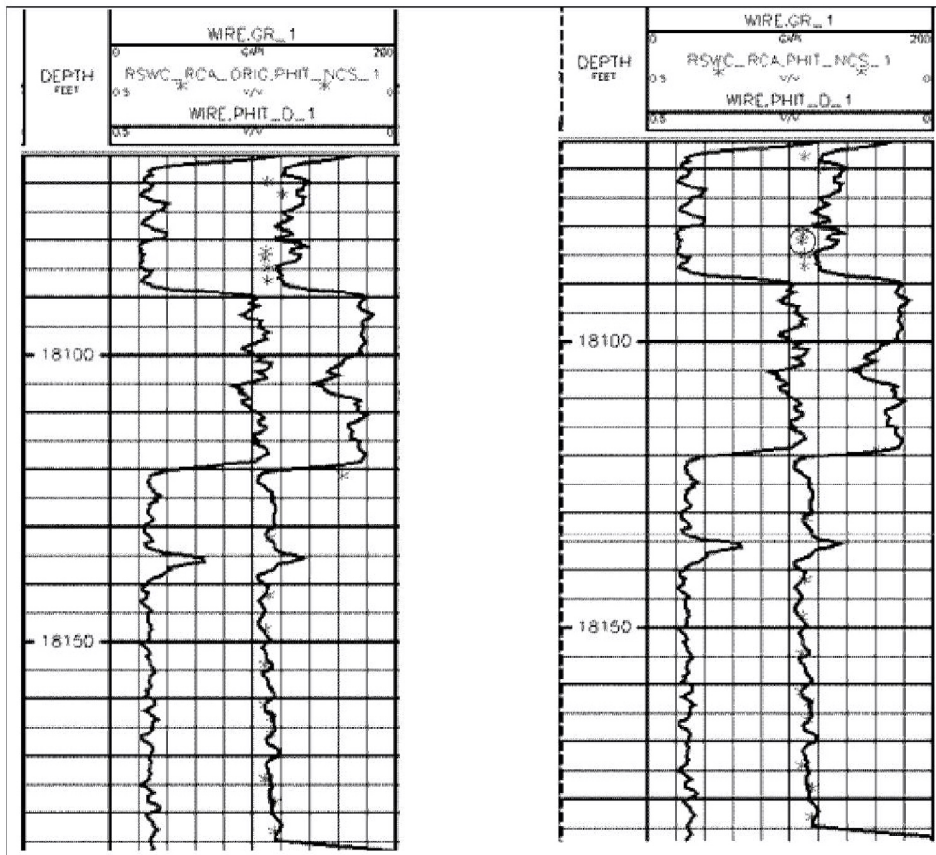


Figure 17: Calibration Logs to core. Core porosity at NCS overlays with Density log derived porosity. Original sidewall core plug depths on the left plot, depth shifted plugs on the right.

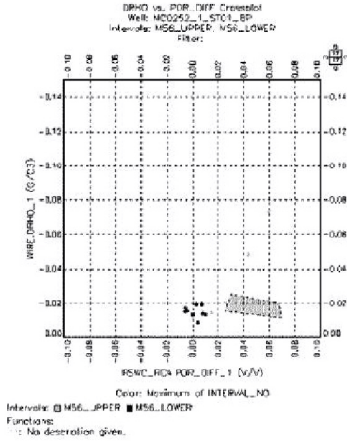
Porosity calculated from density log in upper lobe (M56D) is 2-6 porosity units lower than core derived porosity while in the lower lobe (M56E) they match well.

One of the possible reasons for this mismatch is overcorrecting of the density log (RHOB) for barite additives to mud. The degree of correction (DRHO log) is shown by the red shading in Figure 18.

On the left side in Figure 18a, DRHO (Y axis) is plotted versus the difference between core porosity and density derived porosity (X axis). For M56E sand (in blue) the difference is +/- 1 porosity unit while density correction DRHO is around -0.015 g/cc; For M56D sand (in green) the density correction and the porosity difference are higher for most of the samples.

The large DRHO corrections match spikes in the PEF curve indicating the greatest barite effect (blue curve in Neutron-Density track) in Figure 18b.

Density correction (DRHO) vs. difference between Core porosity and log porosity.



If Upper sand was affected by barite as Lower sand DRHO should be -0.015 g/cc

Density correction (DRHO) vs. difference between Core porosity and log porosity.

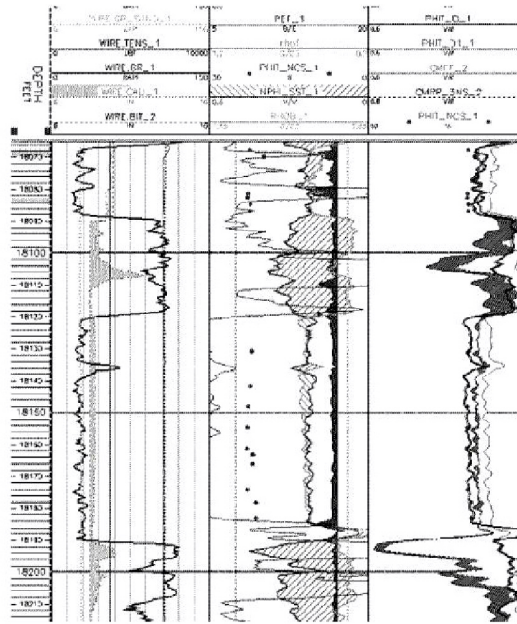


Figure 18a and Figure 18b: Density log correction in M56D.

To eliminate the over correction, DRHO values ≤ -0.015 were replaced by -0.015 and Rhob in upper sand M56D log was corrected and used for density porosity calculation.

After the correction was made, the Density porosity (Phit_Upper) matched Core porosity more closely and the extrapolated fluid density matched much closer to the fluid density of 0.845 g/cc, estimated in M56E. As the reservoir fluids in both reservoirs are very similar and the mud filtrate is the same this is a reasonable outcome (Figure 19).

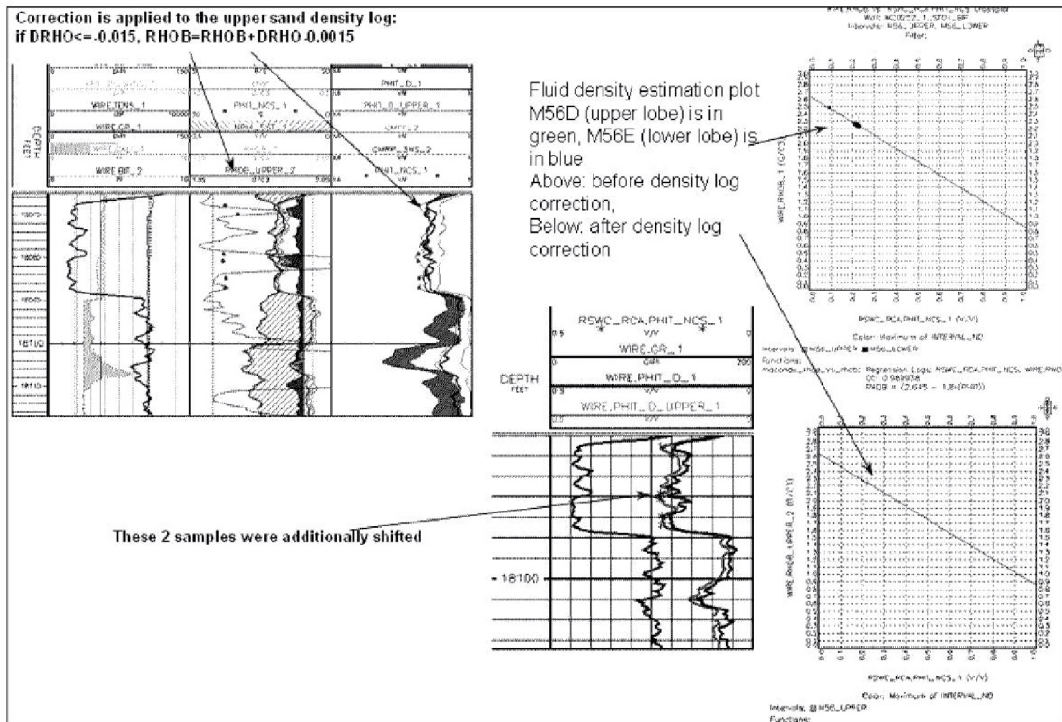


Figure 19: Overlaying Density porosity in M56D with core porosity and cross plots of corrected Density log with core porosity for Fluid density estimation.

The need to make this correction to tie the core data suggest a slightly higher uncertainty in petrophysical parameters in the M56D sand compared to the M56E sand.

There may be other factors to take in to consideration such as anisotropy due to thin beds.

Permeable intervals

Volume of shale (Vsh) cut-off was used to identify permeable intervals.

Gamma Ray log was used for Vsh estimation. For VSH calculation GR_sand and GR_shale lines were created and Vsh was derived as:

$$Vsh = (GR - GR_{sand}) / (GR_{shale} - GR_{sand})$$

The sand and shale lines were adjusted to reflect the sand percentages from the mudlog and Quartz volume estimated by of ECS log.

For identifying all possibly permeable layers a Volume of shale (VSH) cut-off of 0.4 is used.

The cumulative sand count for each of the permeable sands is presented in Figure 20.


	TOPS_SAND TVD_1	TOPS_SAND TVDSS_1	TOPS_SAND FORMATION_1	TOPS_SAND SUM_GROSS_SAND_
17467.0000	17456.07351	17381.07351	M57B	2.00000
17469.0000	17458.07347	17383.07347		
17700.0000	17689.07027	17614.07027	M57C	8.50000
17708.5000	17697.57014	17622.57014		
17804.0000	17793.06826	17718.06826	M56A	2.50000
17806.5000	17795.56821	17720.56821		
17975.5000	17964.56328	17889.56328	M56B	5.00000
17989.5000	17978.56256	17903.56256		
18030.0000	18019.06017	17944.06017	M56C	2.00000
18032.0000	18021.06004	17946.06004		
18067.0000	18056.05774	17981.05774	M56D	22.00000
18089.0000	18078.05618	18003.05618		
18120.0000	18109.05382	18034.05382	M56E	69.50000
18191.0000	18180.04842	18105.04842		
18217.5000	18206.54683	18131.54683	M56F	6.50000
18238.5000	18227.54573	18152.54573		

Figure 20: Cumulative sand thickness per sand unit.

Petrophysical parameters calculations

Determination of net sand cut off

A frequency histogram of Density porosity is presented in Figure 21. A net sand cut off of 14 % porosity and < 0.4 Vsh was used. These values are based on Gulf of Mexico analog Middle Miocene wells. There is not enough core data to confirm these parameters with permeability distributions.

The Density porosity was compared to Core porosity in the M56D and M56E sands, where rotary sided wall derived porosity was used for calibration (Figure 21). The match between the porosities is characterized with a correlation coefficient 0.862.

In spite of an apparent slight gas signature on Neutron-Density log and CMR porosity being lower than Density porosity (usual for gas sands), fluid sampling of both reservoir sands showed volatile oil, therefore no gas correction was applied to the Density log.

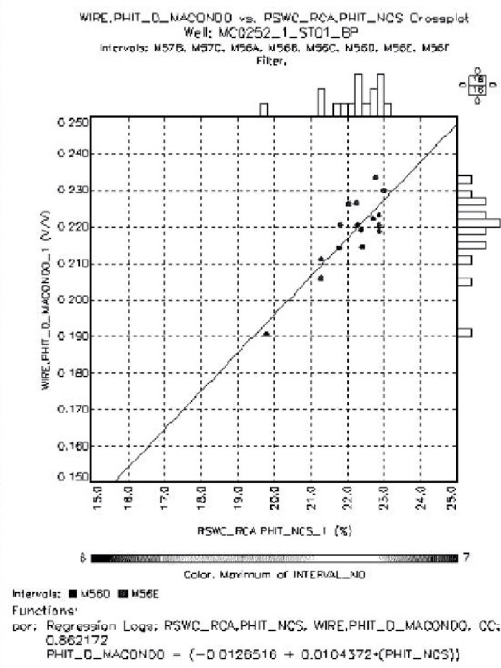
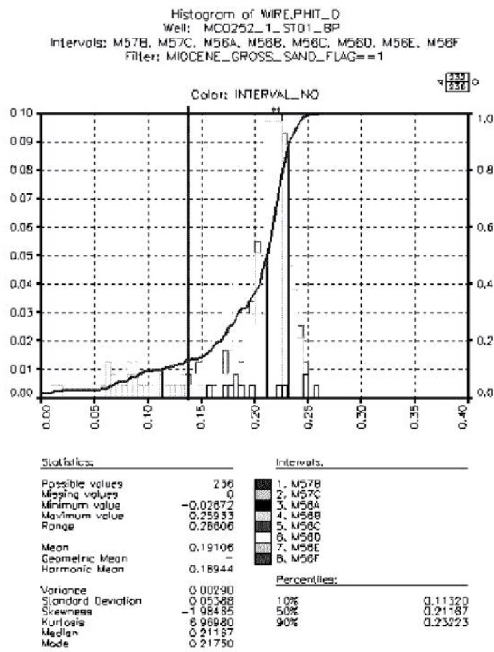


Figure 21: Density porosity histogram with 14% cut off and cross-plot of Core vs. Log derived porosity (with corrected density in M56D).

The Density porosity distribution in the M56E net sand was compared to Core porosity and presented in Figure 22. It shows a good match in minimum, maximum and most likely values suggesting that the rotary sidewall cores taken were not biased towards either more porous and permeable or less porous and permeable zones, and are representative of the bulk formation or at least of the net sand. The same histograms of porosity in M56D do not show such a good match using log porosity derived from uncorrected density as discussed above (Figure 23).

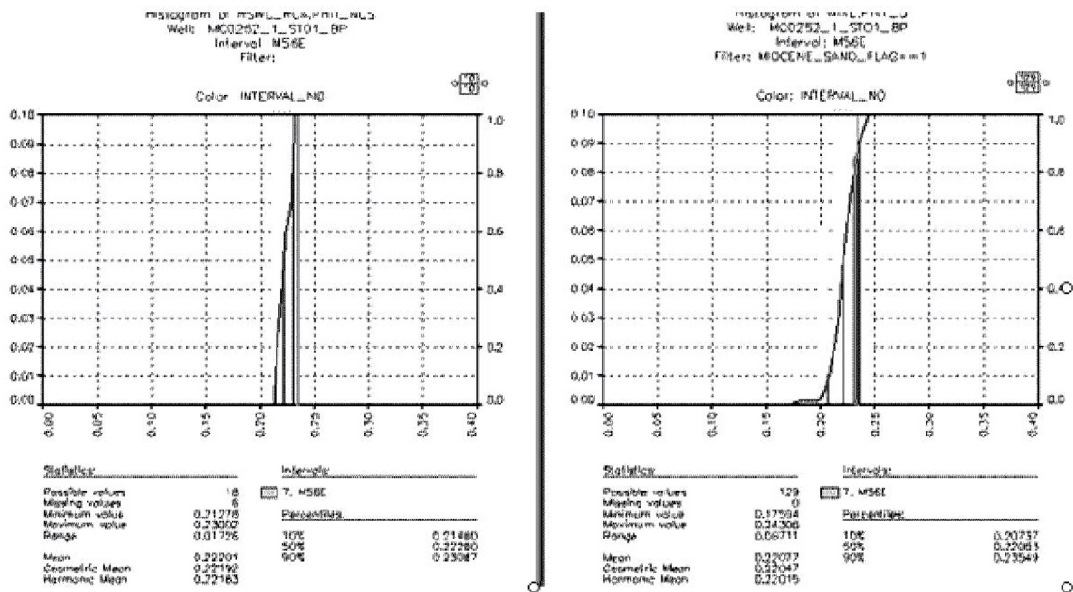


Figure 22: Core porosity (left) and Density Porosity distribution in M56E sand. The red lines represent the 10, 50 and 90 percentiles.

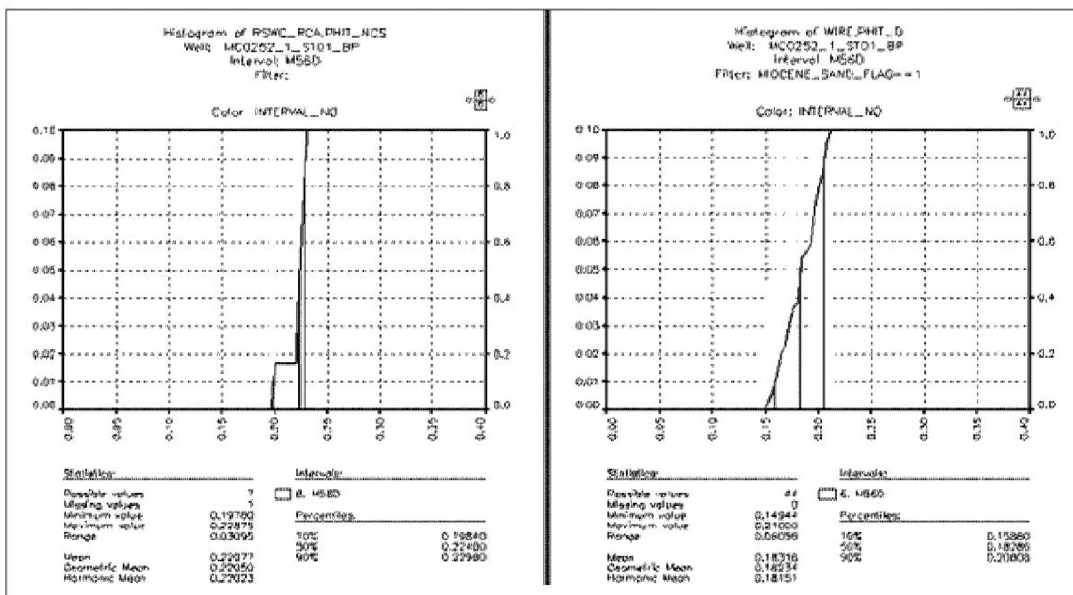


Figure 23: Core porosity (left) and Density Porosity (with uncorrected density input) distribution in M56D sand. The red lines represent the 10, 50 and 90 percentiles.

If the corrected density is used in the M56D sand for porosity calculation the comparison with core data is closer (Figure 24).

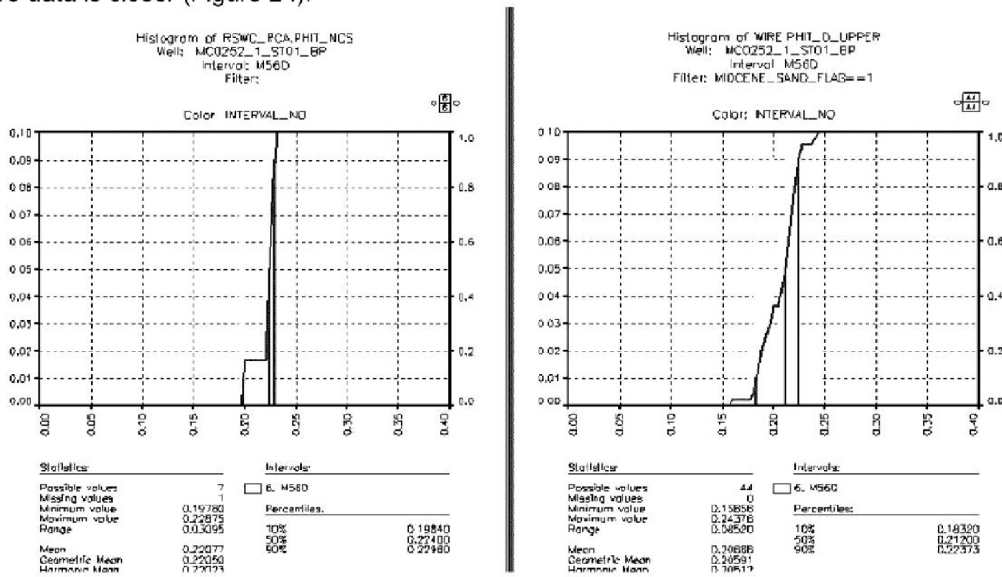


Figure 24: Core porosity (left) and Density Porosity (with corrected density input) distribution in M56D sand. The red lines represent the 10, 50 and 90 percentiles.

Three further sands have been identified in the TD hole section, which have a probable gas signature on Neutron-Density logs: namely M57B, M56A and M56F. No core samples were taken in the M57B and M56A sands though one sample was taken in M56F and is currently under evaluation. Fluid typing of the sands is uncertain and parameters are difficult to assess accurately due to the thin nature of these sands, being below confident log resolution. At this point of interpretation no gas correction applied to the Density porosity in these sands

Water Saturation (Sw)

No thick aquifer sand was observed in the interval of evaluation to determine Rwa.

An assumed regional value of Rw of 0.021 Ohmm at a bottom hole Temperature of 243°F from control data was used for Sw evaluation.

The Archie parameters; a=1, m=1.81 and n=1.88 from the Isabella well were used as an analog for Sw calculation. They were determined from Special Core Analysis on rotary side wall cores plugs from the Isabela well.

The Sw evaluation will be re-visited after Electrical properties and Mercury Injection Capillary Pressure measurements are finished. Sw is a subject to some uncertainty currently.

Frequency histograms of Sw are presented in Figure 25. A conservative estimate of 50 % Sw cut off for pay was used in this evaluation. The cut off value will be revisited after SCAL results are available. SCAL program is planned to include capillary pressure measurements in conjunction with resistivity index measurement to derive drainage fluid distribution and irreducible water saturation (Swi). The histogram in Figure 25 shows a bi-modal saturation distribution and this is also reflected in the permeability distribution in Figure 15. Both sands are considered at irreducible water saturation, however it will be confirmed by completing the air-brine capillary pressure program.

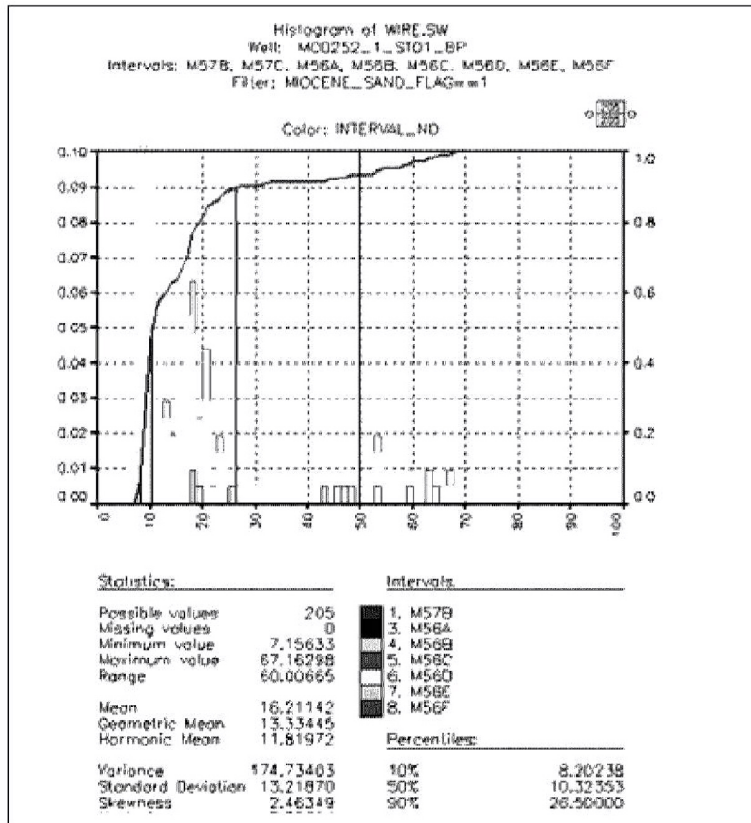


Figure 25: Water saturation Sw histogram with Sw=50% cut off. The red lines are 10, 50 and 90 percentiles.

Permeability

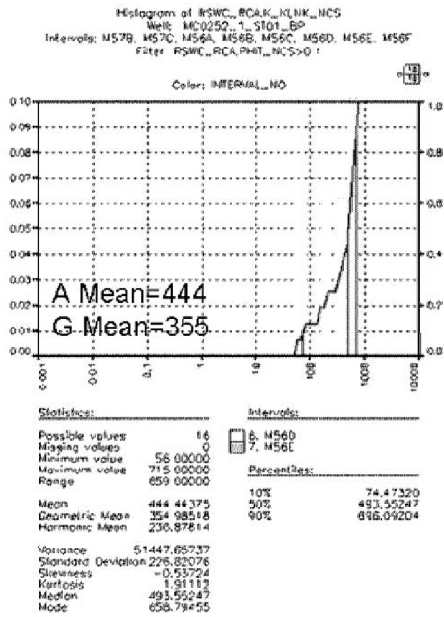
Permeability (to air) was calculated using core derived equation of:

$$K=10^{*(-6.23958 + 0.396339*(PHIT_D*100))}$$

Where PHIT_D is density porosity in v/v

Core derived permeability in the M56D and M56E net sand was compared to Log derived permeability and presented in Figure 26. It shows reasonable match in geometric and arithmetic mean values. Log permeability was derived from uncorrected density porosity.

CORE:



LOGS:

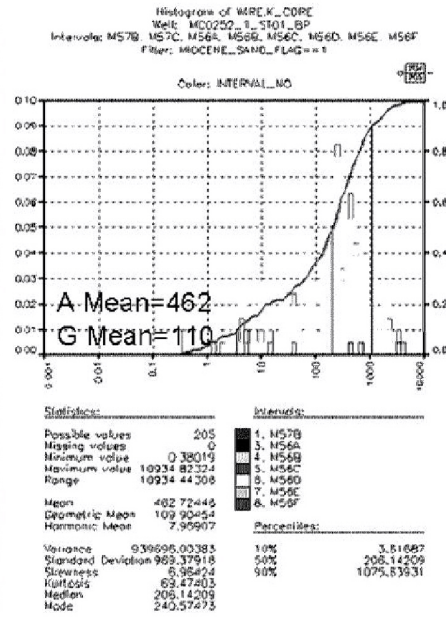


Figure 26: Core derived (on the left) and Log derived Permeability

However if the corrected density porosity is used for log permeability calculation, the geometric average of log permeability matches better to core derived, see Figure 27.

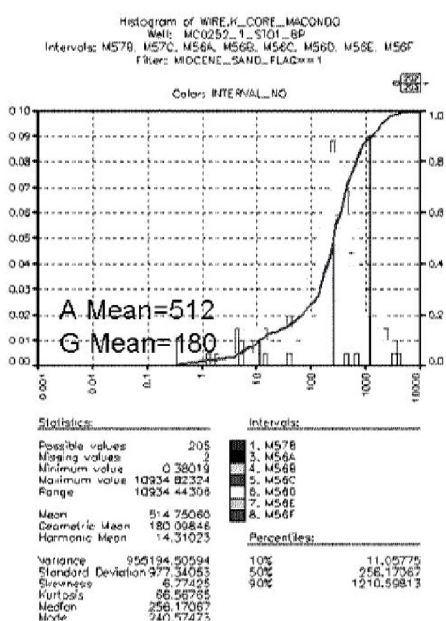
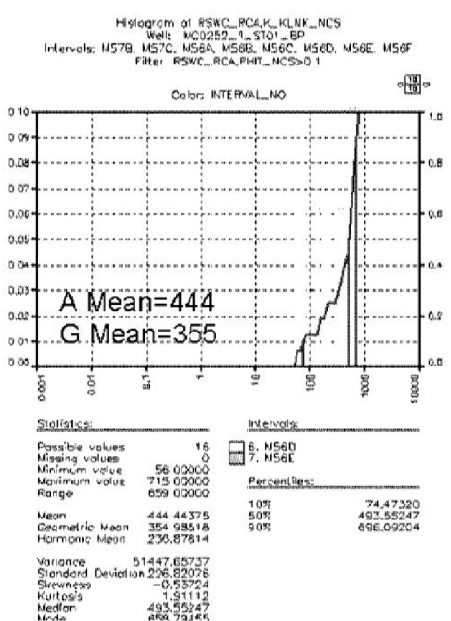


Figure 27: Core derived (on the left) and Log derived Permeability with corrected density log input.

The cross plot of the core measured and log derived permeability matches with $R^2=0.59$. The low correlation coefficient is due to a low amount of data, as we have 17 core plugs of less than 1" to describe 90' of reservoir. The cross-plot is presented in Figure 28.

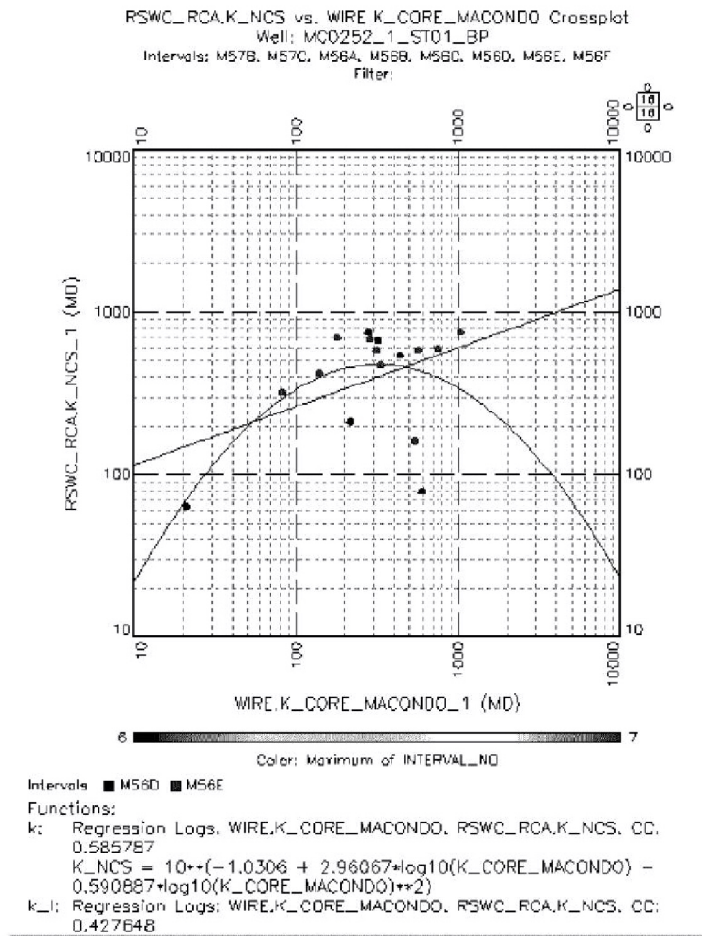


Figure 28: Log derived Permeability (X-axis) vs Core derived permeability (Y-axis). Correlation coefficient=0.59.

Fluid Interpretation

Based on MDT pre-test pressure data analysis and fluid sampling analysis, the M56D and M56E reservoirs comprise volatile oil with GORs of around 3000 with an API gravity of 35. A more complete set of data and analysis will be presented in the Fluid Properties section.

The M56F sand underlying the main pay zone was not sampled by the MDT tool but based on its location below M56D and M56E and below the thermogenic front it is likely to be oil.

The fluid analysis of the M57B and M56A sands is uncertain (Figure 29). Sand M56A has a sonic log signature similar to M56D and M56E, which are oil bearing sands. Sonic porosity calculated in the sand matched density porosity, which also an evidence to be oil sand as Sonic porosity is usually higher than density porosity in gas sand. There was no gas heavier than C1 observed on mud gas chromatograph in the M57B and M56A sands and neither cut or florescence on cuttings. However, based on the M56A position right above the boundary of thermogenic front, it could be gas (see Figure 37).

The M57B sand is approximately 2 feet thick and is below log resolution for accurate fluid determination. However, if hydrocarbons were present, based on the neutron-density cross-over and its position above the thermogenic front it is likely to be gas rather than oil.

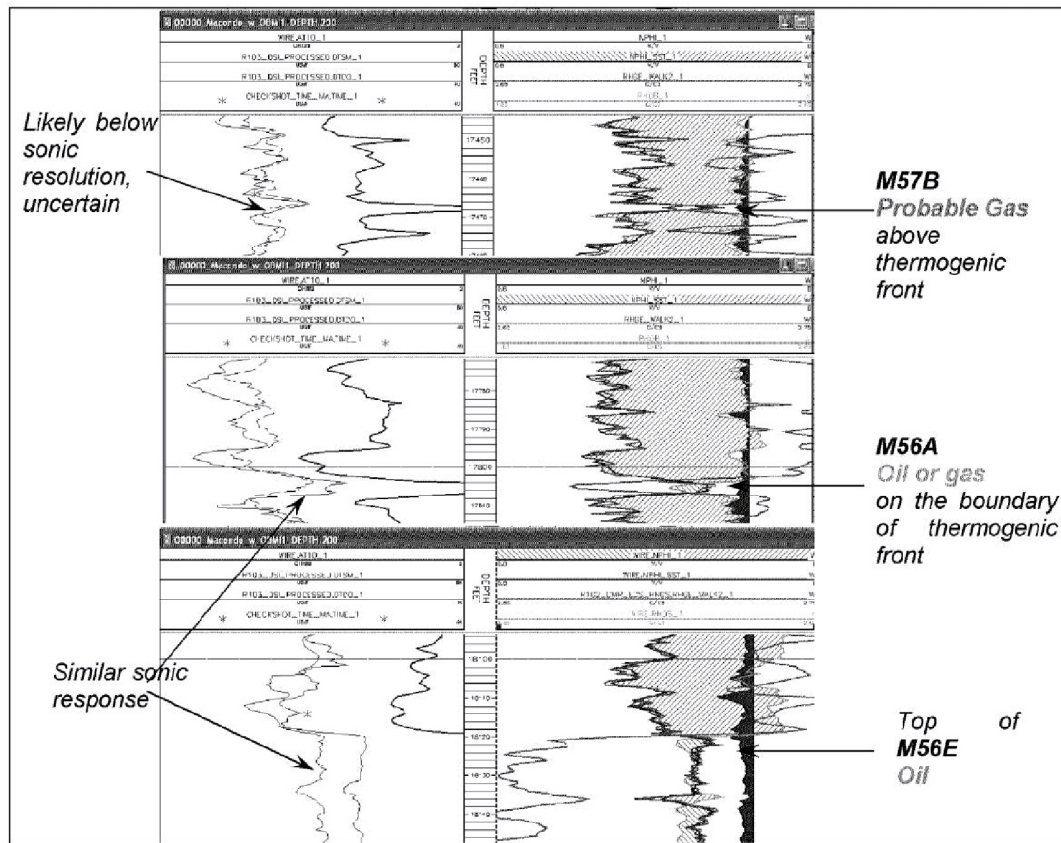


Figure 29: Fluid typing of sands M57B and M56A.

During the initial analysis at the well site, the M57B sand was not interpreted as gas bearing. The interpretation was based on logs field print presented in Figure 30, where the M57B lacks the pronounced neutron-density cross-over as observed in the gas bearing M56A sand. In addition there was no mud gas response over M57B.

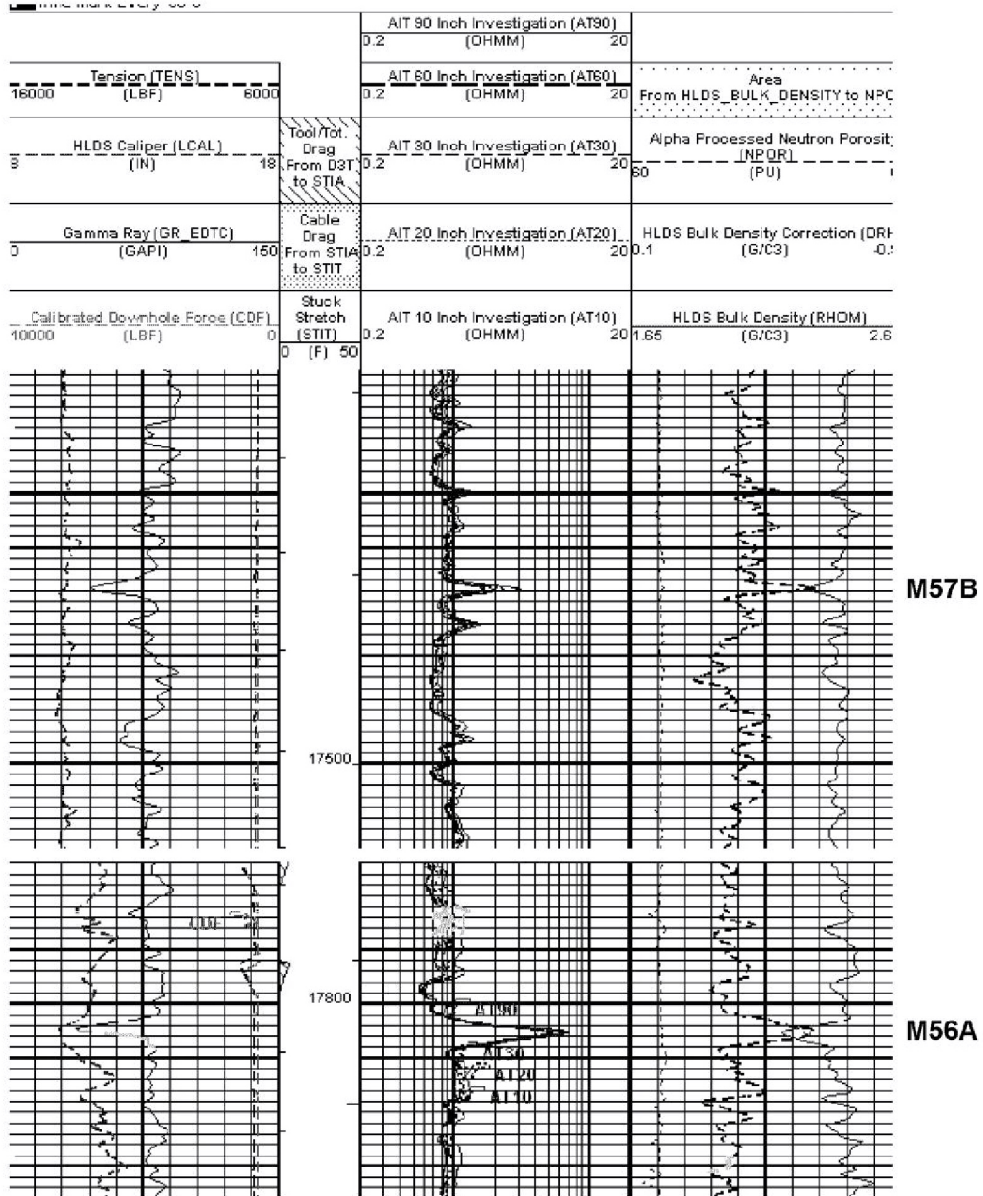


Figure 30 Triple Combo field print over M57B and M56A.

The Schlumberger ELAN well logs analysis shows the M57B saturation is moved water (i.e. the elevated resistivity is due to synthetic mud invasion), see Figure 31.



Figure 31 Schlumberger ELAN analysis over M57B and M56A

A pressure reading of 14.19 ppg was obtained in the M57C Sand (17,700' MD) using logging while drilling (LWD) real-time Geotap tool. During formation evaluation testing, MDT pressure readings in this sand failed to seal. The geotap test of 14.19 ppg was deemed acceptable and can not be disregarded. The OBMI image suggests that the sand is very thinly interbedded (Figure 32). The thin sand stringers are below density log resolution so the evaluation of porosity, Sw and fluid type is compromised.

There are several more thin (<1 ft) sand or silt stringers, characterized by slightly decreased density and slightly increased resistivity values such as those at 17437.5', 17450', 17474' md. The stringers properties are below conventional logs resolution and their lithology and fluid type are uncertain.

Sand M56B is interpreted to be a thin, low porosity water-bearing sand. Sand M57C is interpreted to be a thin, low porosity sand of uncertain saturation.

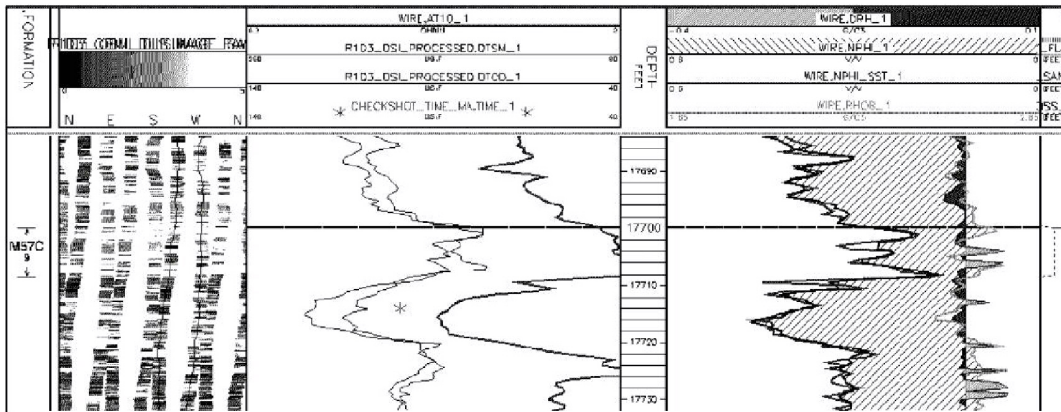


Figure 32: Logs over sand M57C.

Reservoir and fluid quality

Despite limited core data availability, the integration of the core, log and pressure data suggests that:

- Both M56D and M56E sands have good reservoir quality and reservoir fluid.
- Based on XRD data, the M56D and M56E sand lobes have similar mineralogical content with Quartz content averaging 93% and with only minor amounts of clay and secondary minerals (Figure 13).
- Sorting, grain size and sand content are the main controls on reservoir quality.
- From Core data, two rock types have been identified; M56E comprises mainly Rock type 1 and is differentiated from Rock Type 2 by improved sorting. The rock Types are also identifiable in K/Phi space with an average pore throat radius of 10 microns dividing the Rock types. The M56D sand comprises both Rock type 1 and 2. Rock type 1 maybe associated with a more homogeneous sand package; Rock Type 2 in the M56D unit may be associated with some thin bedded pay as evidenced by increased anisotropy from the tensor resistivity data and the CMR bin porosity distribution. There is a better match between core porosity and permeability in Rock Type 1 of the M56E sand than exists for the more heterogeneous sands of M56D and therefore less uncertainty on reservoir

parameters. Thin section data will be integrated with the rest of the data when available to strengthen these assumptions.

- Mobilities from MDT pre tests confirm the two sands have high permeability in the 100's of millidarcy range.
- Figure 33 shows the permeability estimation from different data.
 Red symbols – permeability measured on core (to air),
 Brown line – permeability calculated from Density porosity using core derived equation (see underestimation of Permeability in M56D).
 Red line was used for averages instead – permeability with corrected Density porosity input.
 Blue symbols – drawdown mobilities from MDT pretests,
 Green symbols – draw down mobility from MDT samples.
 Drawdown mobility is a rough estimate of permeability to oil.
 Pretests mobility does not look valid to use, MDT samples mobility multiplied by 0.17 cp viscosity can be compared to Permeability to air measured on core and calculated with logs – magenta stars.
- There is a good match of log derived porosity K_CORE and CMR derived KTIM (purple curve).
- Three fluid samples were obtained – one in M56D and two in M56E. All three samples identified the same fluid type - volatile oil with GOR ~3000 and API=35°. The three samples have contamination below 1.2% of mud filtrate which is considered high quality.

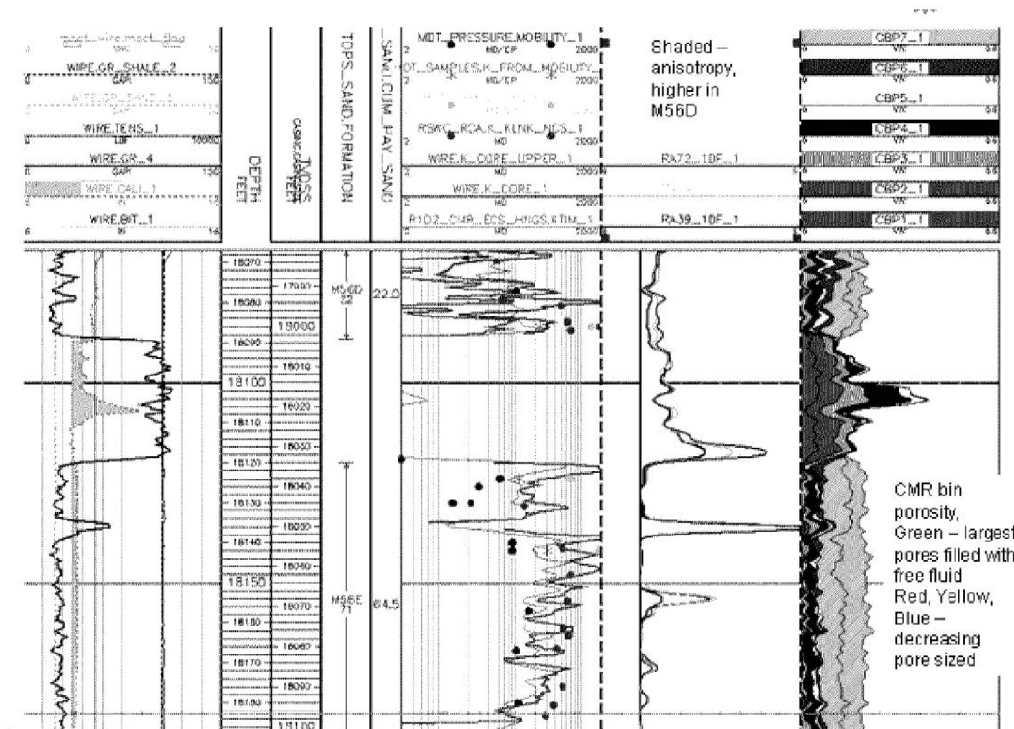


Figure 33: Log data demonstrating M56D and M56E analysis.

- Pressure gradients are presented in Figure 34. Sample and MDT points show very slight different gradients between the two sands (0.249 psi/ft and 0.251 psi/ft for M56E and M56D respectively) but they were taken with different probes that may explain the difference.

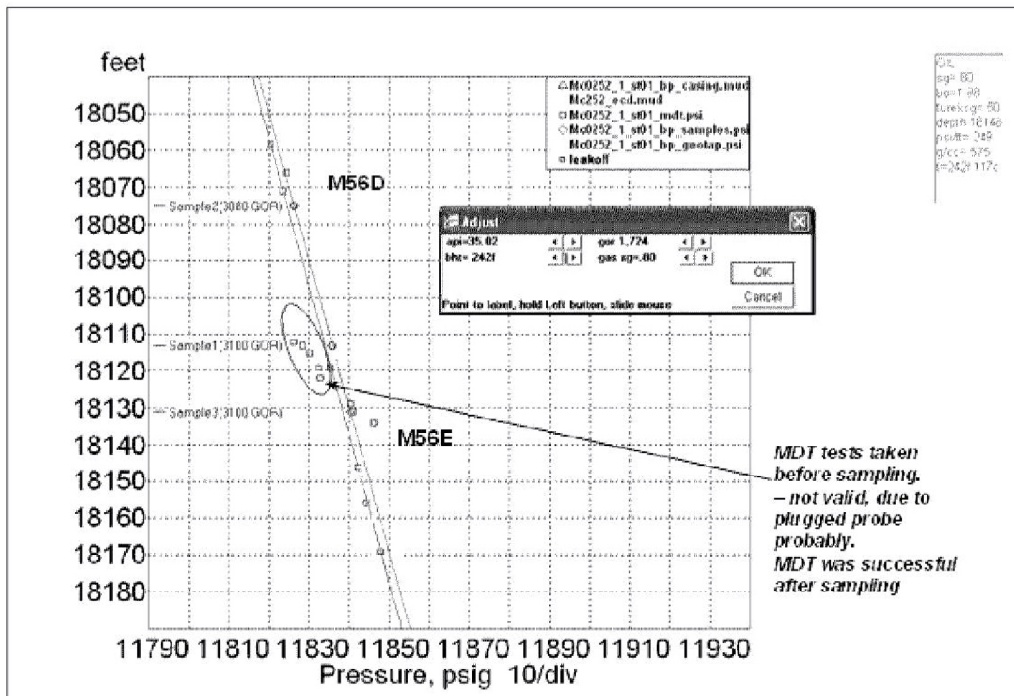


Figure 34: Presgraf pressure plot.

Net/Pay summary

A summary of the gross, net and pay sand is presented in Figure 35. For M56D corrected Density porosity, Sw and Permeability are used for averaging.

Top of Sand MD Depth Feet	Bottom of Sand MD Depth Feet	Top of Sand TVDSS Depth Feet	Bottom of Sand TVDSS Depth Feet	Fluid Content	Sand Name	Gross Sand Feet	Net Sand Feet	Pay Sand Feet	Average Gross Porosity %	Average Net Porosity %	Average Pay Porosity %	Average Net Sw %	Average Pay Sw %	Arithmetic Air Perm MD	Geometric Air Perm MD
17467.0	17469.0	17381.1	17363.1	Probable Gas	M57B	2	2	2	18.0	18.0	18.0	52	52	15	8
17700.0	17708.5	17614.1	17622.6	Uncertain	M57C	8.5	0	0	9.0						
17804.0	17806.5	17718.1	17720.6	Oil or Gas	M56A	2.5	2.5	2.5	22.5	22.5	22.5	24	24	1702	457
17975.5	17989.5	17889.6	17903.6	Brine	M56B	5	3	0	14.2	17.0		58		7	3
18030.0	18032.0	17944.1	17946.1	Brine	M56C	2	2	0	17.3	17.3		64		5	4
18067.0	18089.0	17981.1	18003.1	Oil	M56D	22	22	22	20.7	20.7	20.7	17	17	258	102
18120.0	18191.0	18034.1	18105.0	Oil	M56E	69.5	64.5	64.5	21.4	22.1	22.1	9.7	9.7	514	324
18217.5	18238.5	18131.5	18152.5	Oil	M56F	6.5	6.5	6.5	21.1	21.1	21.1	22	22	1441	130

Figure 35: Macondo net/pay summary table.

Petroleum Systems and Fluid Properties

Temperatures (pre- versus post-drill)

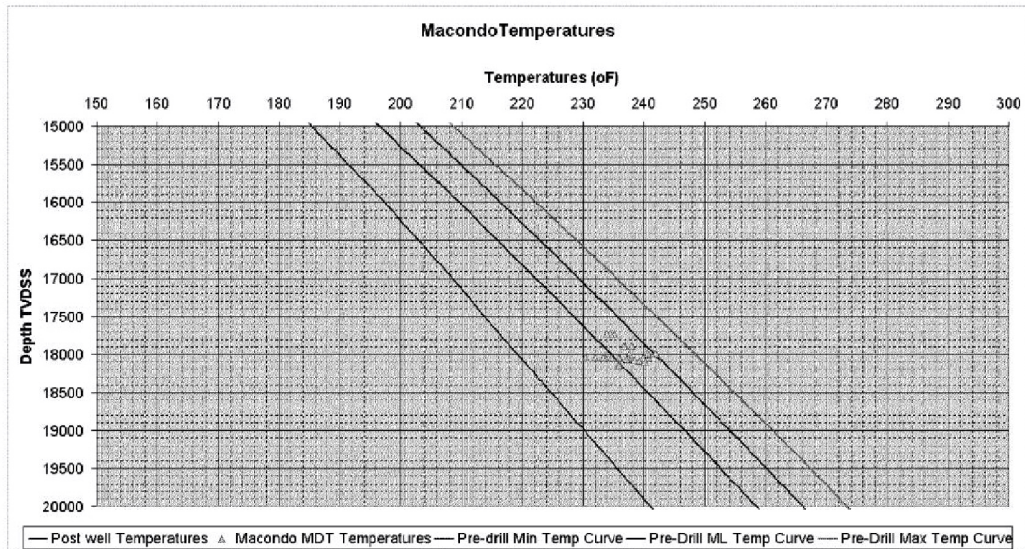


Figure 36: Pre- versus Post-drill temperature comparison.

The reservoir temperatures were predicted to be in between 219 and 248 °F, with a most likely case at 235 °F. The post well temperatures, acquired from the MDT tool gave a broad range between 230 and 242 °F (Figure 36). Therefore the post-drill temperature range was similar to the pre-drill temperature prediction.

The black curve is the post-well temperature curve. It takes into account the outer limit of the MDT temperatures as the closest reservoir temperature reading.

The post-well temperature curve is slightly above the most-likely pre-drill curve (~7 °F) but is close to the pre-drill temperature prediction. The 7 °F temperature difference should not impact the rest of the subsurface interpretation.

Headspace & Isotope (Reservoir zone)

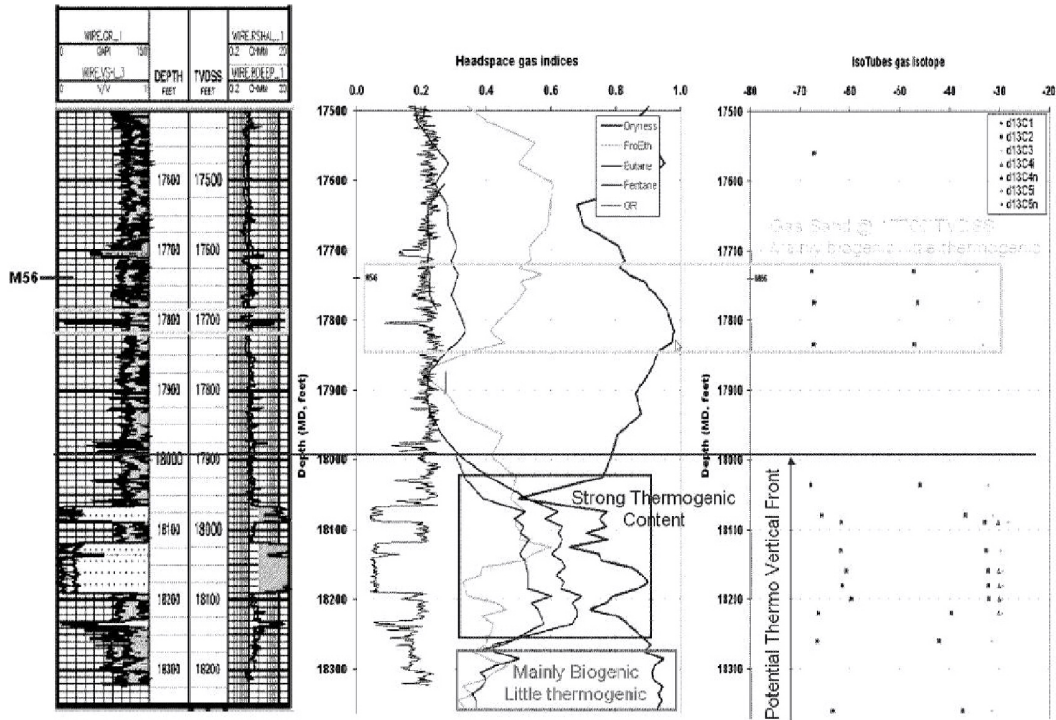


Figure 37: headspace gas indices and isotope results from isotubes.

Using the headspace gas indices and isotope results from isotubes, the thermogenic vertical front appears at 18000' MD (17900' TVDSS) (Figure 37). Indeed, the pro-ethane, butane, and pentane indices increase drastically, while the dryness index severely decreases. Moreover, the methane isotopes appear less depleted and the butane isotopes become present.

The base of the well (below 18250' MD / 18150' TVDSS) has more a biogenic signature. It is believed that the vertical thermogenic front does not pass exactly by the wellbore, giving the idea of a lateral charge. However, it is certainly a vertical thermogenic front.

The section shallower than 18000' MD (~17900' TVDSS) has a strong biogenic signature with some rare amount of thermogenic hydrocarbon. However, it is mainly biogenic gas. The sand at 17800' MD (17700' TVDSS) is a good example: it is mainly biogenic methane, but has a small amount of ethane and propane coming from the thermogenic charge. This charge was lateral in nature.

Fluid properties

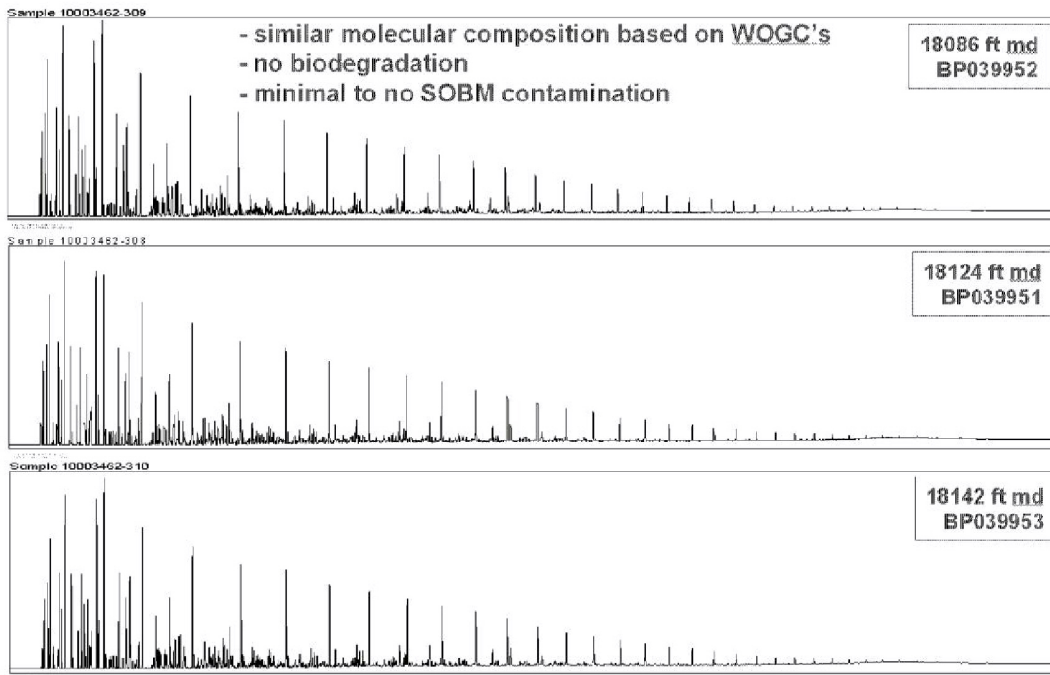


Figure 38: Chromatograms for the three dead oil samples derived from the 3 fluid samples.

Three fluid samples were taken at the level of the reservoir zone: one sample in the M56D sand (upper sand lobe at 18086' MD / 17999' TVDSS), and 2 samples in the M56E sand (middle sand lobe at 18124' and 18142' MD / 18037' and 18055' TVDSS).

Three dead oil samples were derived from those 3 fluid samples and were analysed for whole gas chromatography. The chromatograms are shown in the Figure 38.

By comparing the three chromatograms, we can conclude that the 3 oil samples have a very similar molecular composition, that there is no biodegradation and a minimal contamination level from the drilling mud.

By looking at the headspace and isotube concentrations as well as the isotope signatures, we can also conclude that the M56D, M56E, and M56F sands are oil and have similar composition. The M56F sand (18250' MD) is oil but has a higher content of biogenic gas than the M56D and M56E sands.

MDT fluid samples were taken at three depths. These are the volumes that were obtained during sampling.

Sample Depth	2 ¾ gallons	MPSR	SPMC
18086' MD	1	4	2
18124' MD	1	4	2
18142' MD	1	6	0

The three samples were tested offshore for quality assurance. The results from a single flash are summarized below.

Sample Depth	Contamination	Gas-Liquid Ratio (scf/stb)	Liquid API	Gas Gravity	Reservoir Pressure (psi)	Temperature (F)
18086' MD	1.2 wt %	3017	34.9	0.7823	11841.04	241.9
18124' MD	<1.0 wt %	2909	34.7	0.8050	11850.41	242.3
18142' MD	<1.0 wt %	2840	35.0	0.7837	11855.83	242.6

After samples were brought back to shore, the MPSRs were restored for 5 days to reservoir pressure and temperature.

From flash liquid composition all three zones are equivalent in signature (Figure 39).

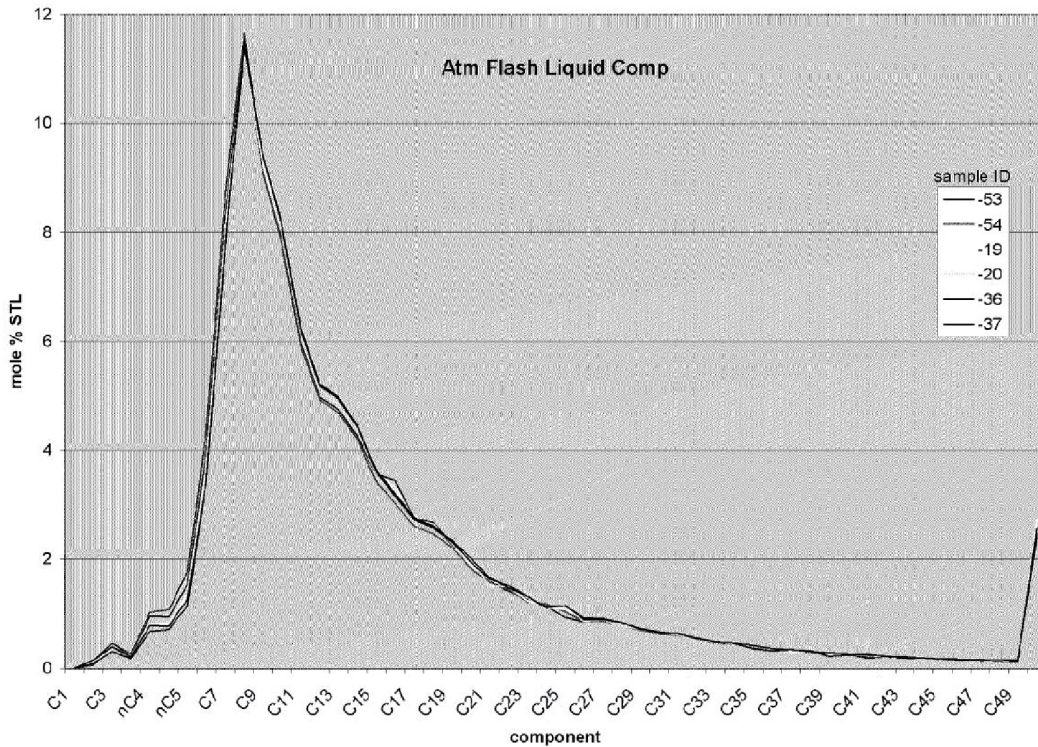


Figure 39: Flash liquid composition comparison.

Three separate labs, Pencor, OilPhase, and Westport, conducted independent tests. Testing conducted at the labs (Note: not all labs did the same tests) are single-stage flash, viscosity and density measurements, constant composition expansion, differential liberation, multi-stage separator test, mini-assay, asphaltene onset pressure, and wax appearance test. Below is a summary of the measured results conducted by the labs at different sample depths. Full PVT reports are available.

PVT Properties	Pencor (Core Lab)	Oilphase (Schlumberger)	Westport (Intertek)	Sample Depth (MD, ft)
Saturation Pressure (psia) at Reservoir Temperature	6,504	6,348	6,438	18,142
Saturation Pressure (psia) at Reservoir Temperature	6,500	N/A	N/A	18,124
Saturation Pressure (psia) at 100F	6,636	6,235	6,107	18,142
Saturation Pressure (psia) at 100F	6,640	N/A	N/A	18,124
GOR (scf/stb), Single-Stage Flash	2,810	2,945	2,831	18,142
GOR (scf/stb), Single-Stage Flash	3,056	3,096	N/A	18,086
GOR (scf/stb), Single-Stage Flash	2,890	2,994	N/A	18,124
API, Single-Stage Flash	35.2	34.6	35.6	18,142
API, Single-Stage Flash	34.8	34.7	N/A	18,086
API, Single-Stage Flash	34.7	34.6	N/A	18,124
Oil FVF (rb/stb) at Saturation Pressure, Single-Stage Flash	2.564	2.539	2.510	18,142
Oil FVF (rb/stb) at Saturation Pressure, Single-Stage Flash	2.618	N/A	N/A	18,124
GOR (scf/stb), Separator Test	2,554	2,442	2,747	18,142
GOR (scf/stb), Separator Test	2,485	N/A	N/A	18,124
API, Separator Test	38.2	37.4	37.4	18,142
API, Separator Test	38.3	N/A	N/A	18,124
Oil FVF (rb/stb) at Saturation Pressure, Separator Test	2.367	2.262	2.388	18,142
Oil FVF (rb/stb) at Saturation Pressure, Separator Test	2.339	N/A	N/A	18,124
Oil Density (g/cc) at Initial Reservoir Conditions	0.587	0.590	N/A	18,142
Oil Density (g/cc) at Initial Reservoir Conditions	0.583	N/A	N/A	18,124
Oil Viscosity (cp) at Initial Reservoir Conditions	0.168	N/A	0.260	18,142
Oil Viscosity (cp) at Initial Reservoir Conditions	0.203	N/A	N/A	18,124
Asphaltene Onset Pressure (AOP, psia) at Reservoir Temperature	N/A	9,500	N/A	18,086
Asphaltene Onset Pressure (AOP, psia) at Reservoir Temperature	N/A	6,615	N/A	18,124
Wax Appearance Temperature (F) at 4,200 psia	N/A	80.0	N/A	18,142
Dead Oil Wax Appearance Temperature (F)	89	N/A	N/A	18,142
Dead Oil Wax Appearance Temperature (F)	N/A	92.5	N/A	18,124
Dead Oil Wax Content (wt%)	N/A	1.77	N/A	18,124